Strål
säkerhets
myndigheten
Swedish Radiation Safety Authority

Author: James Penfold

Technical Note

2014:55

Further Reproduction of SKB's Calculation Cases and Independent Calculations of Additional "What If?" Cases

Main Review Phase

Report number: 2014:55 **ISSN:** 2000-0456
Available at www.stralsakerhetsmyndigheten.se

SSM perspektiv

Bakgrund

Strålsäkerhetsmyndigheten (SSM) granskar Svensk Kärnbränslehantering AB:s (SKB) ansökningar enligt lagen (1984:3) om kärnteknisk verksamhet om uppförande, innehav och drift av ett slutförvar för använt kärnbränsle och av en inkapslingsanläggning. Som en del i granskningen ger SSM konsulter uppdrag för att inhämta information och göra expertbedömningar i avgränsade frågor. I SSM:s Technical note-serie rapporteras resultaten från dessa konsultuppdrag.

Projektets syfte

Det övergripande syftet med projektet är att ta fram synpunkter på SKB:s säkerhetsanalys SR-Site för den långsiktiga strålsäkerheten hos det planerade slutförvaret i Forsmark. Det specifika syftet med detta uppdrag är att förstå SKB:s kapselbrottsberäkningar genom att reproducera de så kallade ”what if” fallen och ”rest” scenarierna för att illustrera hur de tekniska barriärerna fungerar.

Författarens sammanfattning

Som en del av säkerhetsanalysen SR-Site presenterar SKB modellresultat som illustrerar kapseln och buffertens säkerhetsfunktioner. I var och en av de fem beräkningsfallen är delar av kapsel och/eller buffert frånvarande i modellen av slutförvarssystemet. Modellresultaten jämförs inte med säkerhetskriterier eftersom beräkningsfallen innehåller extremt konservativa antaganden.

Inom detta uppdrag har en oberoende reproducering gjorts av SKB:s beräkningsfall och resultaten har granskats, för att ge SSM ett oberoende perspektiv på den roll som barriärerna i närområdet kan tillhandahålla för säkerheten. Analysen innebar användning av SKB:s underlag för att återskapa radionuklidtransportmodellerna med en annan datorkod; AMBER. En betydande del av tolkning och anpassning behövde göras för att uppnå detta, både för att klargöra aspekter av SKB:s modeller och för att bestämma den bästa metoden för att reproducera dem.

Jämförelsen mellan beräkningsresultat från AMBER och från SKB:s modeller begränsades av det lilla urval av resultat som SKB presenterar för de aktuella fallen. Men AMBER gav ändå resultat som överensstämde väl med SKB:s beräkningar, oftast med en faktor inom intervallet 2-5.

SKB:s modelleringsresultat tyder på att de viktigaste faktorerna som kontrollerar hur slutförvarssystemets fungerar är:

- kapselns integritet,
- bränsleomvandlingshastighet och radionukliders löslighet, som styr frisättningen av radionuklider från en skadad kapsel,
- den effektiva hastigheten för utsläpp från buffert till bergssprickor (ekvivalent flödeshastighet) och
- matrisdiffusion i geosfären.

Den viktigaste aspekten av förvarets konstruerade system är kapselns integritet. Resultaten indikerar att det viktigaste kravet på bufferten är att skydda kapseln genom att begränsa flödet av grundvatten över dess yta. Ytterligare en iakttagelse är att, förutom kapseln, har de inneboende egenskaperna hos avfallet (bränsleomvandlingshastighet) och den geologiska miljön (sprickegenskaper och geokemi) nyckelroller vad gäller radionuklidutsläpp från närområdet.

I jämförelse med närområdet visar beräkningarna att geosfären ger relativt lite skydd som barriär mot radionuklidutsläpp, förutom för sorberande radionuklider. För dessa radionuklider kan matrisdiffusion ha en märkbar inverkan på hastigheten för transport till ytmiljön.

Projektinformation
Kontaktperson på SSM: Shulan Xu
Diarienummer ramavtal: SSM2011-592
Diarienummer avrop: SSM2014-1148
Aktivitetsnummer: 3030012-4090

SSM perspective

Background

The Swedish Radiation Safety Authority (SSM) reviews the Swedish Nuclear Fuel Company's (SKB) applications under the Act on Nuclear Activities (SFS 1984:3) for the construction and operation of a repository for spent nuclear fuel and for an encapsulation facility. As part of the review, SSM commissions consultants to carry out work in order to obtain information and provide expert opinion on specific issues. The results from the consultants' tasks are reported in SSM's Technical Note series.

Objectives of the project

The general objective of the project is to provide review comments on SKB's postclosure safety analysis, SR-Site, for the proposed repository at Forsmark. The objective of this assignment is to assess SKB's canister failure calculations through reproduction of the so called "what if" cases and "residual" scenarios to illustrate "barrier functions".

Summary by the author

As part of the "SR-Site" safety assessment, SKB presents modelling results that illustrate the safety functions of the canister and buffer. In each of five calculation cases elements of the canister and/or buffer are absent from the model of the disposal system. The model results were not compared with safety criteria as the calculation cases contain extremely conservative assumptions.

These cases have been independently reproduced, and the results examined, to provide SSM with an independent perspective on the role of the near-field barriers in providing safety. The analysis involved using SKB's documentation to recreate the radionuclide transport models in a different computer code, AMBER. A significant amount of prototyping was needed to achieve this, both to clarify aspects of SKB's models and to determine the best method of reproducing them.

The comparison of the AMBER and SKB calculations was limited by the small selection of results presented by SKB for the cases under consideration. Nevertheless, the AMBER model provided results that agreed well with SKB's calculations, usually to within a factor of 2 – 5.

For the model specified by SKB, the results indicate that the key factors that control the performance of the disposal system are:

- the integrity of the canister;
- the fuel conversion rate and elemental solubility, which control the release of radionuclides from a damaged canister;
- the effective rate of release from the buffer into the fracture (the "equivalent flow rate"); and
- matrix diffusion in the geosphere.

The key part of the repository's engineered system to which a degree of reliability and confidence needs to be assigned is the canister. The results indicate that the main requirement for the buffer is to protect the canister by limiting the flow of groundwater over its surface. A further observation is that – with the exception of the canister – the key controls on radionuclide release from the near-field are intrinsic properties of the waste (the fuel conversion rate) and the geological environment (fracture properties and geochemistry).

By comparison with the near-field, the calculations suggest that geosphere offers relatively little as a barrier to radionuclide release, except for sorbed radionuclides. For these radionuclides, matrix diffusion can have a notable influence on the rate of transport to the surface.

Project information
Contact person at SSM: Shulan Xu

Strål
säkerhets
myndigheten
Swedish Radiation Safety Authority

Author: James Penfold I
Quintessa Limited, Warrington, United Kingdom

Technical Note 71

2014:55

Further Reproduction of SKB's Calculation Cases and Independent Calculations of Additional "What If?" Cases

Main Review Phase

Date: September, 2014
Report number: 2014:55 **ISSN:** 2000-0456
Available at www.stralsakerhetsmyndigheten.se

This report was commissioned by the Swedish Radiation Safety Authority (SSM). The conclusions and viewpoints presented in the report are those of the author(s) and do not necessarily coincide with those of SSM.

Contents

1. Introduction

Strålsäkerhetsmyndigheten (SSM, the Swedish Radiation Safety Authority) is reviewing the "SR-Site" safety assessment developed by Svensk Kärnbränslehantering AB (SKB, the Swedish Nuclear Fuel and Waste Management Company). SR-Site is a central element of a licence application for a final repository for Sweden's spent nuclear fuel, located at Forsmark.

SSM has concluded that SKB's reporting is sufficiently comprehensive and of sufficient quality to justify a continuation of SSM's review to the main review phase. The main review phase is focused on tasks and issues prioritized by SSM in order to judge the compliance of the application with SSM's requirements. This includes detailed analysis of a range of specific issues by independent experts. This report describes such one such analysis, undertaken by Quintessa on behalf of SSM.

The objective of the study was to assess SKB's calculations that consider so-called "what if" cases and "residual" scenarios which explore the role of the near-field barriers in providing safety. The key engineered barriers are the canister and the buffer, and SKB have defined five cases that illustrate their function by selectively removing them from the analysis. The calculation cases are simply intended to illustrate aspects of the disposal system's performance and are not, therefore, representative of a plausible set of conditions. This study involves seeking to reproduce the calculations undertaken by SKB in order to provide insight into all the assumptions, model descriptions and parameter values behind the calculations. This will then inform SSM's judgment on this aspect of SKB's safety case. Some additional calculations have also been undertaken to explore aspects of SKB's assessment, such as the dependence of model results on particular parameters. Because the "what if" scenarios defined by SKB are intentionally extreme and limiting in nature, additional calculations focus on exploring modelling assumptions rather than scenario definition.

The report is structured as follows. Firstly, the models and data that have been used for the calculations are described in Section 2. These have all been derived from SKB documentation or supporting, detailed documents supplied on request by SKB. This is followed in Section 3 by a description of the calculation approach that has been taken, again based on the specifications provided by SKB. Implementation of the models and data requires some iteration in order to find the best interpretation of the modelling approach, and this "prototyping" stage is described in Section 4. Results are presented in Section 5, with a summary of key issues in Section 6 and conclusions in Section 7.

2. Model

2.1. Modelling Approach and Codes

2.1.1. SKB's Approach

A variety of mathematical approaches can be used to represent the models presented by SKB in its radionuclide transport report; however, it is most appropriate to adopt a mathematical approach similar to that used by SKB in order to explore the calculations in detail. SKB's suite of codes is described in Section 3.6 of SKB (2010a) and includes:

- COMP23, a compartment modelling code (written in Matlab/Simulink) used for radionuclide migration calculations in the near-field (the canister and engineered system);
- FARF31, which uses a Laplace solution to the advection-dispersion equation to model transport in a one-dimensional "streamtube", coupled with representation of diffusion perpendicular to the advective flow to represent matrix diffusion; and
- MARFA, a Monte Carlo simulation of the transport of radionuclides in fractured or unfractured geologic media, represented with a particle-based approach.

These codes also use the results from supporting calculations (e.g. using the ConnectFlow code) to parameterise various aspects such as the groundwater flow characteristics and geochemistry. Reproduction of the supporting modelling is beyond the scope of this project.

2.1.2. Approach in this Study

The focus of the study is on reproducing the radionuclide transport calculations undertaken by SKB, in particular the characteristics of the near-field, as described in the five calculation cases used by SKB to illustrate barrier function:

- A - An initial absence of sufficient buffer in deposition holes;
- B - An initial pinhole in the copper shell for all canisters;
- C - An initial, large opening in the copper shell and cast iron insert of all canisters;
- D - A combination of cases A and C (an initial large opening in all canisters and absence of buffer);
- E - A combination of case C with an assumption of fast fuel dissolution and fast corrosion of metal parts (complete in only 100 years).

The priority is to suitably represent the the near-field model, therefore it is necessary that a compartment modelling approach is used for this aspect of the assessment. The far-field can also readily be represented using a compartment modelling approach. As combination of the near-field and far-field models offers the benefit of analysing the system with a single, integrated model, this approach has been

adopted. A summary of the key features of compartment modelling is presented in Appendix 2.

2.1.3. Modelling Code

Compartment modelling is a well-established mathematical approach and there is a range of software applications available in which compartment models can be implemented. As well as Matlab/Simulink, used by SKB, codes frequently used in safety assessments include AMBER and GoldSim. For this study, the AMBER code has been selected (Quintessa (2013a)). The code has a long track record of application to radionuclide transport modelling associated with geological disposal, including in support of regulatory reviews.

- AMBER has previously been used to support regulatory review studies of geological disposal programmes by SSM (and their predecessors) and STUK (e.g. Maul et al. (2008));
- The code has been applied to geological disposal in various countries (see Little et al (2011), Walke and Paulley (2009), Little et al. (2007 and 2003)).

Although AMBER has been used previously to independently model SKB's disposal system, no existing models have been used in this study. In order to check that they are fully described by SKB, all aspects of the models described in this report have been developed directly from SKB's documentation (SKB 2010a; SKB, 2010b).

AMBER is managed and developed within a quality assurance system that is accredited to the ISO 9001:2008 standard and which explicitly incorporates the requirements of the TickIT software development scheme (Quintessa, 2013b, c, d). AMBER releases are benchmarked against a suite of verification tests (Quintessa, 2013e) and has been validated through numerous international code intercomparison exercises, for example Maul et al. (2003, 2004), Jones (2004), Andra (2003).

The code incorporates all of the features required to represent the near- and far-field radionuclide transport process, including corrosion and fuel conversion (represented with release rates), advection and dispersion. AMBER also allows non-linear processes including the capability to restrict the amount of contaminants that are available for transfer from compartments and thus model solubility limitation. The code includes robust time-stepping and Laplace solvers and features the automated selection of optimum time-steps, which can avoid numerical problems resulting from the inappropriate or inflexible specification of time-steps. Finally, AMBER is fully probabilistic, with users being able to choose from a range of probability distribution functions, full Monte Carlo and 'stratified' Latin Hypercube sampling options. Parameter distributions generated with other codes can also be used because of AMBER's capability to read data from ASCII "sample files".

Models in AMBER are generated by the user through the specification of parameters (which can include equations and data) and networks of compartments and transfers. The code is very flexible, and any number of parameters, transfers and compartments can be specified. In addition, AMBER supports the exchange of data between software codes, enabling data to be imported from supporting calculations undertaken in other codes.

All AMBER models are fully transparent - there are no predefined constraints on the modelling approach to be used. This makes the resulting models easy to review and audit. All of the model information is included in text-based case file.

Figure 1: Example of an AMBER Model

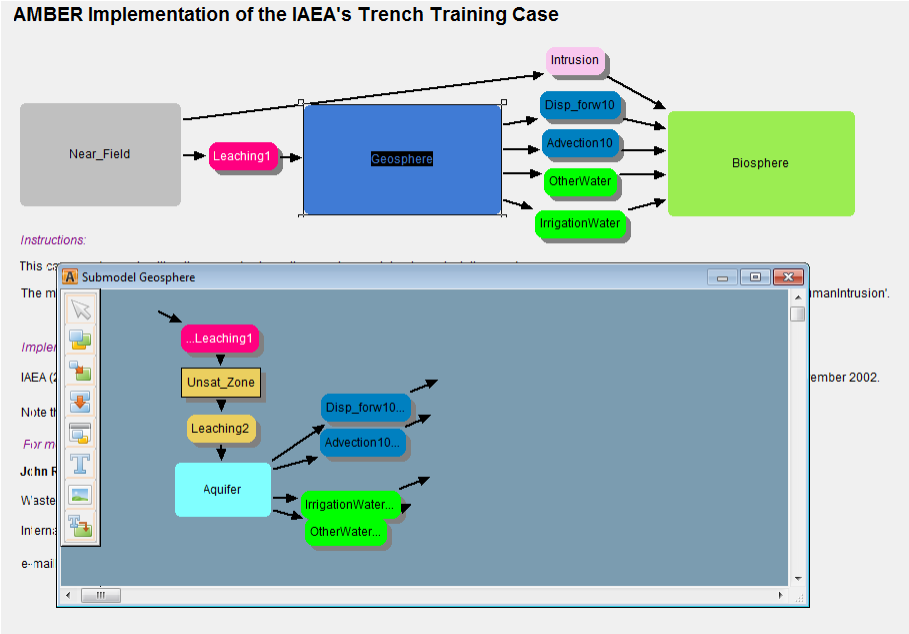

2.2. Key Model Components

SKB (2010a) summarises information on the models and data used in its assessment, whilst SKB (2010b) provides a detailed description of the data selected. These sources of information form the basis of the models implemented in the AMBER code. Appendix G of SKB (2010a) provides a particularly useful description of the near-field models. The following subsections summarise the way in which these have been implemented in AMBER. Further details of the approach to specific calculation cases are presented in Section 3, and a description of the process of optimising the model is presented in Section 4. Illustrations of the model structure, and a summary of key parameters and the sources of data used, are presented in Appendix B.

2.2.1. Canister

Model Structure

The canister is represented by four compartments, each of which represents a distinct part of the canister and fuel in which the radionuclides may be present. The compartments are:

- *FuelMatrix* – the fuel itself and associated fission and activation products;
- *Cladding* – irradiated fuel cladding and associated radionuclides;
- *CanVoid* – the void space in the canister, which will fill with groundwater after the canister is breached; and
- *Hole* – the fluid-filled hole in the canister through which contaminants are released into the buffer

Transfers between these components represent the time-dependent release of radionuclides from the fuel and cladding. A transfer between the *FuelMatrix* and *CanVoid* represents the release of contaminants from the fuel conversion. A transfer between the *Cladding* and *CanVoid* represents the corrosion release of contaminants from the fuel cladding.

Transfers between *CanVoid* and the buffer are via the *Hole* compartment in the case of a pinhole, or directly from *CanVoid* if the hole is large. This represents the transport of contaminants into the buffer as a result of a defect or hole in the canister, and releases only take place after the defect occurs.

Release from the Fuel

A fraction of the inventory is assumed to be instantaneously released into the canister void. This is represented by partitioning the initial inventory of each radionuclide between the compartments, *FuelMatrix, Cladding* and *CanVoid*. The initial amount of radioactivity in the canister void is:

$$I_N^{Void} = I_N \ IRF_N$$

Where

I_N is the total inventory of radionuclide *N* in the fuel (mol, defined in Table 3-7 of SKB (2010b)), and

IRF_N is the instantaneous release fraction for radionuclide *N* (unitless).

Radionuclides are subsequently released from the fuel into the void both by corrosion and fuel conversion. Thus, the initial amount of radioactivity in the *FuelMatrix* is

$$I_N^{Fuel} = I_N \ (1 - IRF_N - CRF_N)$$

And the initial amount in the *Cladding* is

$$I_N^{Clad} = I_N \ \ CRF_N$$

Where

CRF_N is the corrosion release fraction for radionuclide *N* (unitless), i.e. the fraction assumed to be associated with cladding.

Parameter value distributions for the IRF_N are defined in Table 3-15 of SKB (2010b). These are implemented as specified (i.e. as point values, normal distributions, and "double triangle" distributions). Each value of CRF_N is sampled using a triangular or "double triangle" distribution, which are specified in Table 3-14 of SKB (2010b). This fraction is released at a uniform rate over a timescale t_{Corr} (y), which is a sampled parameter using a log-triangular distribution with minimum 100 y, maximum 10,000 y and peak of 1,000 y (from Table 3-18 of SKB (2010b)).

Corrosion does not start until after the canister is breached, t_{Delay} (y). After this time, until the cladding is fully corroded (after time t_{corr}), congruent release from the Cladding compartment is represented with a time-varying rate defined by λ_N^{Corr}:

$$\lambda_N^{Corr} = \frac{\tau_{Corr}}{(1 - \tau_{Corr}(t - t_{Delay}))}$$

Here, $\tau_{Corr} = 1/t_{Corr}$, with a value depending on the case being calculated (see Section 4.2.10 of SKB (2010b)).

Release from the fuel is represented by fuel conversion. The fuel conversion rate is specified explicitly as a parameter λ_{FCR} and is a fixed rate per year, independent of

radionuclide. The parameter is defined as a log-triangular distribution with minimum of 10^{-8} y^{-1}, maximum of 10^{-6} y^{-1} and peak of 10^{-7} y^{-1} (distribution is specified in Table 3-21 of SKB (2010b)). Fuel conversion only occurs after the initial delay (t_{Delay} in y).

Release via the Hole

Radionuclide release via the hole is modelled using the concept of transport resistance (denoted generally with *r* and units of y m^{-3}). The expression for the transfer rate is:

$$\lambda_N^{Hole} = \frac{1}{V\, r_N^P}$$

where

V is the volume of the canister void (1 m^3, from Table 4-4 of SKB (2010b));
r_N^P is the diffusive resistance of the hole in the canister (y m^{-3}).

Note that porosity is not included in the term above as the canister void is assumed to fill with water, and there is no retardation applied in the canister as no sorption substrate is modelled. The general term for the transport resistance of the hole r_N is taken from equation G-1 of SKB (2010a):

$$r_N^P = \frac{1}{\pi\, L_{Hole}\, D_N^e \sqrt{2}}$$

where

L_{Hole} is the radius of the hole (m);
D_N^e is the effective diffusion coefficient for radionuclide *N* in the buffer (in m^2 y^{-1}).

The assumptions for the size of the hole, and the time at which occurs and expands is presented in Table 4-7 of SKB (2010b). The radius of the hole (L_{Hole}) is 0.002 m initially (actually 0.001784 m appears to have been used in the modelling, to make the initial area 10^{-5} m^2), before the total area increases instantaneously to 1.0 m^2 at a time t_{Large}.

Parameter distributions for effective diffusion coefficients for the buffer are specified in Table 5-15 of SKB (2010b) and are implemented as triangular or double-triangular distributions in log10-space, as specified by SKB.

Solubility Limitation

The concentration of contaminants in the fluid within canister is limited by the solubility of the contaminants. The AMBER code has the capability to limit the amount of contaminants that can be transferred between compartments to reflect the solubility constraints. To do this is necessary to specify a limit on the total amount of a contaminant in a compartment that is "available" for transport. This is defined for relevant near-field compartments as the maximum amount of an element available for transport, I_E^{Max} (in mol)

$$I_E^{Max} = S_E\ V\ \theta\ R_E$$

where

S_E solubility of element *E* in the groundwater (mol);
V is the volume of the compartment, in m^3;
θ is the porosity (-);

R_E is the retardation of the element in the relevant compartment (-), calculated as described below.

(In the case of the canister, θ and R_E are both equal to unity as the canister is simply a water filled void.) Retardation, $R_{E,}$ is a general parameter, calculated for various media in the modelled system, with

$$R_E = 1 + \frac{\rho\, Kd_E}{\theta}$$

where

ρ is the dry bulk density of the medium (kg m^{-3}); and

Kd_E is the sorption coefficient for element the medium (m^3 kg^{-1}).

Values for the solubility of elements (S_E) are computed and are dependent on the emplacement hole location, taking account of spatial variability. SKB (2010a) (Table 3-4) also give mean values which can be used in calculations which are undertaken for average geometric characteristics.

2.2.2. Buffer and Backfill

Model Structure

Radionuclides released through a defect in the canister will subsequently diffuse through the buffer if it is present. As discussed in Section 6.5 of SKB (2010a), the dominant pathway is the Q1 fracture and therefore this has been the focus of the near-field model. Figure G-3 of SKB (2010a) shows how the section of the buffer between the hole and the Q1 fracture is discretised to model contaminant transport. The buffer is represented with six annular compartments (B1 – B6). The dimensions of the compartments are presented in Table G-2 of SKB (2010a). The discretisation of regions in which diffusion is the dominant transport process is a key consideration. Robinson (2005) discusses how much discretisation is needed to represent diffusive processes within compartment models. In relation to diffusive transport, a measure of the accuracy, when compared with an analytic solution, is that the error resulting from discretisation into a finite number of compartments is equal to the inverse of the number of compartments squared (Robinson, 2005). Consequently, the error from discretisation into a 3-compartment pathway is about 10 % whilst discretisation into 6 compartments results in an error of less than 3%. On this basis, the level of discretisation adopted by SKB is considered to be adequate. The buffer compartments have been implemented in the AMBER model as shown in Figure 2. Each is linked by a forward and backward transfer. Diffusion is represented by transfers in both directions, which simulate the diffusive mixing process. Transfers in the direction from the hole to the fracture also incorporate a term to represent advection (if it is present).

Transport in the axial direction is represented in a similar way, adjusting the dimensions appropriately (using information from Appendix G of SKB (2010a)). An illustration of the whole near-field model structure is provided in Appendix 3.

Figure 2: Compartment Structure in the Buffer/Backfill Sub-model for Transport between the Canister and Q1 Fracture

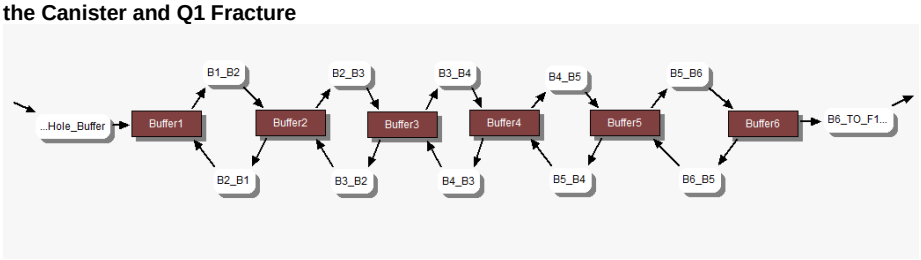

Diffusive Transport through the Buffer and Backfill

The rate of diffusive transport is calculated in the buffer and other parts of the model with the following general equation:

$$\lambda_N^{Diff} = \frac{D_N^e \, A}{L \, C_N}$$

Here,

D_N^e is the effective diffusion coefficient for the material (either buffer or backfill, depending on the compartment in question) in $m^2\ y^{-1}$;

A is the interface area between the compartments from which and into which contaminants diffuse (in m^2);

L is the diffusion distance, taken to be the distance between the centre of adjacent compartments (in m);

C_N is the "capacity" of the donor compartment, in m^3. The capacity of a compartment is defined as:

$$C_N = V \, \theta \, R_N$$

In the case of transport via the hole in the canister to the Q1 fracture, the retarding medium is the buffer, and the geometry is such that diffusion is radially outwards (in the "x" direction of the model). The values for diffusion length and area are taken from Table G-2 of SKB (2010a), whilst the effective diffusion coefficients are as defined in Table 5-15 of SKB (2010b).

For diffusion into the buffer below the hole, and the backfill and backfill above it, then transport is in the "z" direction, and relevant geometry is taken from Appendix G of SKB (2010a).

Data on the density and porosity of the buffer and backfill are given in Tables 5-5, 5-6 and 5-14 of SKB (2010b), whilst the sorption coefficients are presented in Tables 5-17 and 5-19 of SKB (2010b). These correspond to highly saline groundwaters and are cautious.

Advective Transport

The release of contaminants from the diffusive region into a far-field transport pathway (e.g. the Q1 fracture) is modelled as adjective transport with an "equivalent flow rate" (Q_{Eq} in $m^3\ y^{-1}$). The equivalent flow rate is calculated by a detailed model taking into account of the geometry and other characteristics of the interface between the engineered region and the geosphere. The advective transport rate, λ_N^{Adv} (y^{-1}) is calculated with:

$$\lambda_N^{Adv} = \frac{Q_{Eq}}{C_N}$$

The values for Q_{Eq} are calculated with SKB's detailed geosphere model and have been specified for each deposition hole. Median values are also defined for use in deterministic calculations where the spatial variability of the geosphere is not modelled (Table 3-5, SKB (2010a)).

Where the calculation case considers spalling an additional component of equivalent flow, Q_{EqDZ} ($m^3\ y^{-1}$), is included in the numerator. The value of Q_{EqDZ} is calculated based on the assumed geometry of the fracture zone, specified in Equations G-26 and G-27 of SKB (2010). These in turn use the Darcy velocity, U_0 ($m\ s^{-1}$). This parameter is also calculated for each deposition hole, with a median value, suitable for deterministic calculations, specified in Table 3-5, SKB (2010a).

If there is no spalling, an additional component of resistance to transport into the Q1 fracture is included. This is modelled as "plug" resistance similar to that used to represent the hole in the canister. The relevant equation is presented as Equation G.2 by SKB (2010a):

$$r_N^f = \frac{\left(\frac{F_{x,0}}{b}\right) b}{A_f D_N^e}$$

Where

$F_{x,0}$ is the effective diffusion length function (m);
b is the half-width of the fracture aperture (m); and
A_f is the diffusion area, equal to the area of the fracture that intersects the hole (m^2).

The numerator is calculated using an empirical relationship dependent on the dimensions of the fracture and buffer interface. The geometrical factors for two values of fracture aperture that were considered by SKB are given in Table 1, from Section G.2 of SKB (2010a). The larger fracture is taken by default. The additional term included in the transfer to Q1 is therefore $1/(r_N^f\ C_N)$.

Table 1: Geometric Parameters used in the Calculation of the Plug Resistance for the Q1 Fracture

Parameter(s)	Value for fracture of 1 10^{-4} m	Value for fracture of 1 10^{-6} m
A_f (in m^2)	5.5 10^{-4}	5.5 10^{-6}
$\left(\frac{F_{x,0}}{b}\right) b$ (in m)	3.1 10^{-4}	4.4 10^{-6}

2.2.3. Geosphere

Model Structure

Conceptually, transport in the rock mass is represented by advective flow through the fracture system, and diffusion into the rock matrix. In order to represent adequately both advective and diffusive transport in compartmental models it is necessary to discretise contaminant transport pathways into a suitable number of compartments. Robinson (2005) describes the basis for necessary discretisation, and this aspect has been considered in the prototyping calculations presented in Section 4.

The required model structure for each pathway (Q1, Q2 and Q3) is an advective pathway discretised into sequential compartments. With each advective compartment there is an associated a suite of compartments used to represent diffusion into the rock matrix.

Advection in the Fracture

Advection in the fracture can be represented with the following equation.

$$\lambda_N^{Adv} = \frac{q_{Frac}}{L_{Frac}}$$

where

q_{Frac} is the advective velocity in the fracture (m y^{-1});

L_{Frac} is the length of the fracture compartment in the direction of flow (m), equal to the total path length (L_{Geo}) divided by the number of fracture compartments (five, in this case).

Sorption onto fracture surfaces is not accounted for with this expression, but is assumed to be small in comparison with the effect of matrix diffusion and sorption within the rock matrix.

The value of q_{Frac} is calculated from the total fracture path length (L_{Geo} in m) divided by the travel time (T_W in y). Both values are dependent on the spatial variability associated with deposition hole location. A deterministic value for T_W can be obtained from Table 3-5 of SKB (2010a). No equivalent value is available for L_{Geo}, and so an indicative value of 500 m is assumed. The model's transfer rates are not dependent on this parameter therefore the value is nominal.

Matrix Diffusion

Diffusion into the matrix is modelled in the same way as the diffusion through the buffer, with diffusion being assumed to be in the z direction. The effective diffusion coefficient for radionuclides in the rock matrix is defined in Table 6.91 of SKB (2010b).

The thickness of each layer of matrix compartments is derived from the total thickness of the matrix zone, given as 12.5 m in Table 6-85 of SKB (2010b). An adequate representation of diffusion is obtained if each successive layer is about 3 times the thickness of the previous one. For a *m*-compartment system, the thickness of the initial layer, L_M^1 in m, is therefore

$$L_M^1 = \frac{L_D}{\sum_{i=0}^{j} 3^j}$$

The thickness of subsequent layers can therefore be calculated as multiples of this value. The diffusion length between any two rock matrix compartments is then taken to be the distance between the centroids (i.e. half the sum of L_M for adjacent compartments). The length of the matrix compartment is simply L_{Frac} and the width (W_{Frac}) is taken to be 1 m. It is noted that the thick matrix zone (12.5 m) means that even with 6 compartments representing the matrix the first compartment has a size of 3.4 cm; this could lead to an underestimate of the retention effects of the geosphere for sorbed nuclides which do not penetrate the full depth. Because the geosphere is not of primary interest in the current study and the non-sorbed nuclides

are the main contributors to the dose equivalent, this aspect of the discretisation has not been further refined.

3. Calculation Approach

3.1. SKB Calculations

SKB undertakes both probabilistic and deterministic calculations, with the main emphasis being on a probabilistic approach. SKB's probabilistic calculations sample both the uncertainties (in parameters such as sorption coefficients) and spatial variability (e.g. in groundwater flow and related parameters). Where uncertainties are concerned, the number of samples used in a calculation is determined by the required coverage of the probabilistic assessment, but reasonable results can usually be obtained with a few hundred iterations. However, in order to assess spatial variability it is necessary to assess parameters that vary for each individual deposition hole location. In the SR-Site assessment, this requires a total of 6,916 model runs. Not all lead to a release of contaminants to the surface within the assessment timeframe of 10^6 y^{-1} – inspection of the groundwater flow modelling results indicates that only about 1/6 result in a discharge to the surface, as noted in Section 6.5 of SKB (2010a).

The calculation cases examined in this report are described in Section 6.5 of SKB (2010a). These cases are designed to highlight barrier functions rather than provide a simulation of a credible future evolution pathway for the disposal system. The calculations consider various permutations in which one or more near-field barriers are absent. The calculation cases are defined by SKB (2010a) as follows:

- A - An initial absence of enough buffer to cause advective conditions in the deposition hole for all deposition holes.
- B - An initial pinhole in the copper shell which grows after a period of time, for all canisters.
- C - An initial, large opening in the copper shell and in the cast iron insert for all canisters.
- D - A combination of cases A and C, i.e. an initial large opening in all canisters and advective conditions due to loss of buffer for all deposition holes.
- E - A combination of case C with an assumption of fast fuel dissolution and fast corrosion of metal parts. An initial, large opening in every canister is combined with the assumption of complete fuel dissolution and metal corrosion in only 100 years.

Each calculation case was assessed both with and without retention of contaminants in the geosphere. All but one (Case A) involve the canister failing to provide a fully effective barrier from an early time, and are derived from the "growing pinhole" case.

3.2. Approach to the Independent Calculations

The general modelling approach adopted in the independent calculations for all five cases has been described in Section 2. The development and application of these models to specific calculation cases also needs to consider other factors:

- the need to develop the detailed implementation of each case so as to reflect, as near as possible, SKB's calculations; and

- practical limitations to the assessment calculations.

3.2.1. Calculation Case Development

Although the models and data applied by SKB are reported in some detail (SKB, 2010a; 2010b) there is some scope for interpretation as to the specific implementation of the model. For this reason, a significant degree of refinement was expected to be needed during the independent implementation of the models. Rather than seek to refine each calculation case in turn, the approach taken has been to focus on a single case and optimise its implementation to recreate SKB's results, before turning to the other cases.

Taking account of both the range of cases available, and the information (in terms of results) presented by SKB, Case B was selected for the purposes of model development in this study. This case involves the representation of a "growing pinhole". It represents the loss of the canister as a barrier, like Cases C, D, and E. In addition, as well as the failure, by this mode, of all canisters being assessed in Section 6.5 of SKB (2010a), SKB has also analysed the case in Section 6.3 of SKB (2010a) for failure in a single canister. There is consequently a substantial amount of information available against which to compare results, and inform on the model function. The prototyping work to develop the calculation case is presented in Section 4.

3.2.2. Deterministic and Probabilistic Calculations

As noted by SKB, its approach involved a probabilistic analysis of cases A – E in order to ensure that uncertainties were represented. This was possible in part due to SKB's application of an optimised modelling approach for the disposal system which enables runtimes to be minimised. In the independent modelling calculations, it has been necessary to use a general modelling code (in this case AMBER) which offers less scope for minimising runtimes by optimising the underlying calculational code.

Sampled hydrogeological modelling output data, for each of the 6916 realisations, are available separately as data files supplied directly by SKB (2010c). The data files contain values for a range of parameters calculated by the discrete fracture network (DFN) model used by SKB to model groundwater flow. SKB used various approaches to calculate groundwater flow. As stated in Section 6.5 of SKB (2010a), the semi-correlated hydrogeological DFN model was used for the barrier function calculations (correlation refers to the relationship between fracture transmissivity and fracture size). The parameters required for the AMBER implementation of the SR-Site radionuclide transport model include:

- F, the rock transport resistance for Q1, Q2 and Q3 flowpaths (in y/m);
- FLEN, the length of largest fracture that intersects the hole (in m);
- LR_TUN, the path length to the first fracture in tunnel (in m);
- QEQ, the equivalent flow from deposition hole to fracture(s) intersecting deposition hole, for Q 1, 2, 3 pathways (m^3/y);
- TRAPP, the porosity of the transport pathway in the tunnel (-);
- TR_TUN, the travel time of the transport pathway in the tunnel (y);
- TW, the advective travel time through the geosphere for pathways Q1, Q2 and Q3 (in y); and
- U0, the Darcy flux at the deposition hole (in m/y).

Initial investigations with the AMBER implementation of the SR-Site radionuclide transport model indicated that the runtime for an individual realisation, with all radionuclides specified, was typically of the order of 1 minute. With a reduced set of radionuclides faster runs can be achieved (e.g. 5 seconds for C-14 and I-129 only). On this basis, it was practicable to undertake calculations for the full 6,916 realisations considered by SKB (which cover the full set of emplacement holes), but only with a reduced set of radionuclides.

A more practical approach involves sampling only the realisations that lead to a release to the surface. The output of SKB's groundwater modelling calculations contains various "flags" ("OKFLAG", "FPC" and "EFPC") which can be used to identify those realisations which correspond to deposition holes which did not lead to a release. SKB defines the criteria for identifying such cases in in Section 3.7.2 of SKB (2010a). These criteria can be used to screen the geosphere data and reduce the number of realisations for analysis in the study. Realisations excluded were those cases where:

- there was no release due to the absence of a fracture or low velocity (OKFLAG=1) or contaminants would fail to reach the surface in 1,000,000 y (OKFLAG=2, 3 or 4);
- deposition holes have been excluded due to background fractures or deformation zone fractures (FPC>0).
- canister positions are intersected by fractures that also intersect the entire tunnel perimeter (EFPC>4)

Finally, SKB presents median values for use in deterministic calculations (Section 3.7.2 of SKB (2010a)). Taking account of the time constraints of the project, an approach has been adopted in which:

- deterministic calculations were undertaken with the full radionuclide inventory and all calculation cases;
- probabilistic calculations were undertaken for those realisations that lead to a release from a deposition hole, with a reduced set of radionuclides, for all calculation cases;
- full probabilistic calculations have been undertaken for all 6916 realisations, but with a subset of the radionuclide inventory in which only the dominant contaminants are included, and only for a selected calculation case.

3.2.3. Calculation Case Specifications

SKB's description of the five calculation cases have been used to define the main features of the cases considered in this study. On this basis, the specification for the reference calculation cases is provided in Table 2.

Table 2: Definition of Calculation Cases

Parameter	Case A/A*	Case B/B* ^	Case C/C*	Case D/D*	Case E/E*
t_Corr (y) Timescale for corrosion releases	Reference values	Reference values	Reference values	Reference values	100 y
FCR (/y) Fuel conversion rate	Reference values	Reference values	Reference values	Reference values	10^{-2} y^{-1}
t_Delay (y) Time before release into buffer can start.	From probabilistic calculations (84 instances)	1,000 y (pinhole)	100 y	100 y	100 y
t_Large (y) Time after which there is a large breach of canister.	From probabilistic calculations (84 instances)	10,000 y (large hole)	100 y	100 y	100 y
Kd_BB (m^3 kg^{-1})	Sorption of zero (buffer missing)	Reference values	Reference values	Sorption of zero (buffer missing)	Sorption of zero (buffer missing)
Density (buffer, kg m^{-3})	1000 kg m^{-3} (buffer missing)	Reference values	Reference values	1000 kg m^{-3} (buffer missing)	1000 kg m^{-3} (buffer missing)
Porosity (buffer, -)	1 (buffer missing)	Reference values	Reference values	1 (buffer missing)	1 (buffer missing)
De (m^2 y^{-1}) Effective diffusion coefficient	1 10^{-9} m^2 s^{-1} (buffer missing)	Reference values	Reference values	1 10^{-9} m^2 s^{-1} (buffer missing)	1 10^{-9} m^2 s^{-1} (buffer missing)
Kd_Rock (m^3 kg^{-1})	Sorption of zero for "*" cases	Sorption of zero for "*" cases	Sorption of zero for "*" cases	Sorption of zero for "*" cases	Sorption of zero for "*" cases

Note: * Indicates that the case includes a calculation in which retention by sorption in the geosphere is neglected. ^ Case B has been used for prototyping the independent assessment model.

4. Prototyping the Independent Assessment Model

4.1. SKB Results

Case B, selected as the reference case for the development of the independent assessment model, is the same as SKB's "growing pinhole failure" case (Section 6.3 of SKB (2010a)) but considers holes occurring simultaneously in all canisters. Because the only difference is that Case B considers failure in all deposition holes, the deterministic and mean of probabilistic results in Section 6.3 can also be used as a point of comparison with the model being developed. The only difference is that the results in Section 6.3 of SKB (2010a) are:

- Reduced by an order of magnitude (due to the application of the distributed LDF[1] values); but
- Increased by a factor of 6,916 because all of the canisters are assumed to have failed.

SKB presents both results for a single failed canister, using median values for uncertain parameters (Figures 6-11 to 6-14 of SKB (2010a)) and the results of probabilistic calculations (Figures 6-15 to 6-18 of SKB (2010a), which show the mean of all realisations).

4.2. AMBER Development

4.2.1. Near-Field

Calculation Cases

During the development of the near-field model a range of potential methods of representing the system were considered. These reflected different interpretations of the system, as well as simplifications that were examined to determine if the model could be represented, to a reasonable degree of accuracy, with a simpler near-field model than that developed by SKB. The different model designs focused mainly on exploring the degree of discretisation needed in the near-field.

P1: No Representation of Diffusion in Buffer

The simplest approach to modelling the near-field considered was to represent the release from the near-field into a single well-mixed compartment that represents the whole annulus of buffer from the canister to the edge of the deposition hole. This approach does not directly model diffusion through the buffer. This was considered possibly to be a reasonable simplification because, on the timescales of interest to the assessment, diffusion through the buffer will be relatively rapid. In SKB's

[1] Landscape Dose Factors – pre-calculated radionuclide-dependent coefficients that convert a radionuclide flux to a radiation dose rate to a person, on the basis of assumed human land uses and habits. LDF values can be location and climate-dependent.

model, this part of the system was discretised into six annular compartments, with diffusive transfers represented between them.

P2: No Vertical Diffusion
Significant additional complexity to the model is needed for the representation of diffusion perpendicular to the dominant transport pathway (Q1). This requires Blocks 4, 5, 6 7 and 8 to be incorporated in the model (see Appendix G in SKB (2010a)), with associated advective and diffusion transfers. A prototype case was therefore considered as a development of the "No Diffusion in Buffer" case, in which Block 3 was represented in the same manner as SKB, but the other Blocks were absent.

P3: No Solubility Limitation
Solubility limitation is a non-linear process that can significantly influence the time taken to solve a calculation case. This prototype model included all eight Blocks as defined by SKB, but omitted the representation of solubility limitation to test whether it had an important bearing on the results (noting that two key radionuclides, C-14 and I-129, are not solubility limited).

P4: No Back Diffusion through the Hole
When representing diffusive processes it is important to ensure that there are adequately balancing transfers. It is unclear from SKB's model description if there is a balancing diffusive transfer from the buffer back into the canister (or whether it is only release from the canister represented). In order to gauge the importance of this issue, a case was developed which did not represent this balancing transfer.

P5: Reference
The reference case incorporates a full representation of the processes described by SKB, as interpreted in this study, including diffusion through all blocks, advective transport where relevant, solubility limitation and balancing transfers for all diffusive processes.

Comparison with SKB Results

Comparing the different configurations of the prototype AMBER model with SKB's results provides an indication of the scope for simplification of the model, and also demonstrates broadly the sensitivity of the model to the specific implementation of the processes under consideration. The five cases have been shown in Figure 3 and compared with SKB's results for the single canister failure deterministic case (Figure 6-11 of SKB (2010a)).

The highly simplified implementation (P1: no diffusion in the buffer) essentially only represents the release from the hole, and the resistance offered by the Q1 fracture. Whilst this provides clearly different results, the peak dose is only four times greater than SKB's results, and the results are generally within an order of magnitude, except on timeframes of more than 100,000 y, when long lived and sorbed radionuclides that would otherwise be retarded in the buffer are released. The results for all other calculation cases are within a factor of two of at the peak or a factor of three at times after 10,000 y. Solubility limitation can be seen to be important for certain radionuclides (Case P3 does not include the process), but as the dose equivalent releases are dominated by C-14 and I-129 the total dose is not substantially affected (it is increased, largely due to Se-79 which is otherwise solubility limited up to about 1,000,000 y). The results for the case in which all

releases are directed towards the Q1 pathway (P2) also indicate that this pathway is indeed dominant.

The reference case (P5), and that with the simplified representation of canister release (P4), match the SKB results for the Q1 pathway very closely, providing confidence in AMBER implementation of the near-field model for Case B in particular. Although the agreement in the results is still very good for the Q2 pathway, there is less agreement for the Q3 pathway as can be seen in Figure 4. (Note that for this comparison the SKB results have been scaled to the AMBER results, because different LDF factors were used.)

The Q3 pathway represents the release of contaminants via a fracture that intersects the tunnel above the emplacement holes. The pathway is represented by contaminant migration via a section of buffer covering the canister, a layer of backfill, and the backfill emplaced in the tunnel. Migration through the buffer is by diffusion, but an advective component can exist in the tunnel. The AMBER results suggest a more transfer of contaminants via the Q3 pathway, with a significantly lower long-term release via Q3. The specific reasons for this difference could not be established due to a limited range of calculation results available from SKB for this combination of pathway and calculation case.

A comparison of the results for individual radionuclides is presented in Figure 5. In this case, the dose equivalent release is the sum of the fluxes for all pathways (Q1, Q2 and Q3) weighted by the distributed LDF values (i.e. the SKB results presented in Figure 6-12 have been adjusted with the LDF data from Table 3.7 of SKB (2010a)). Broadly, the agreement in the results can be seen to be very good, although some differences are notable.

Figure 3: Comparison of Alternative Approaches to the Near-field Model Implementation – Releases via the Q1 Pathway

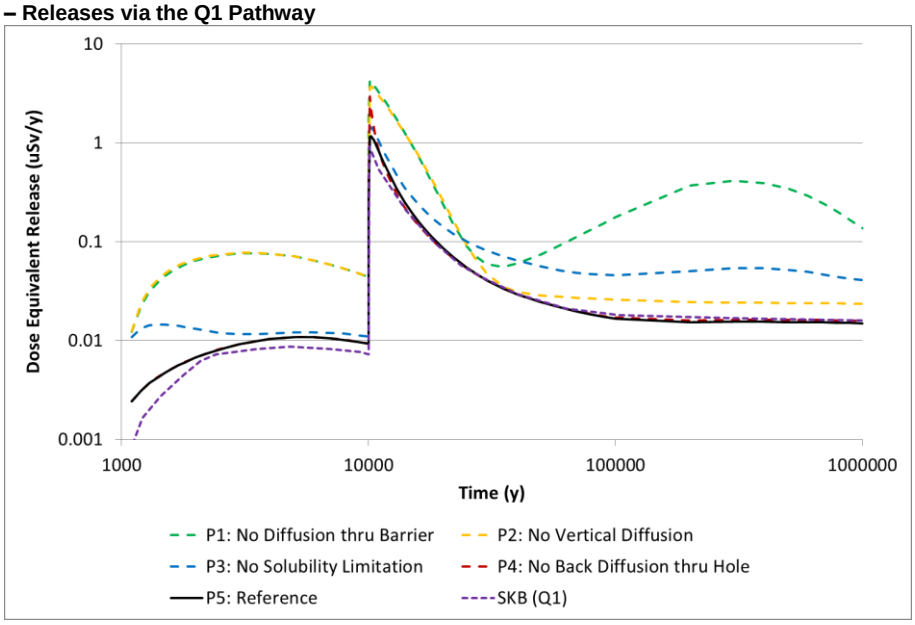

Figure 4: Comparison of the AMBER Reference Near-field Model Implementation with SKB Results for the Q1, Q2 and Q3 Pathways

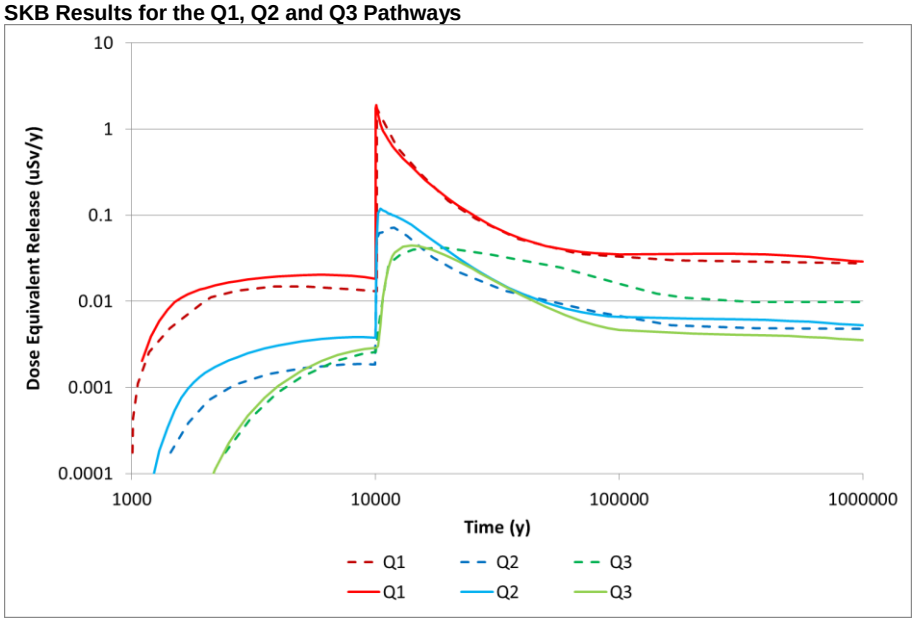

Note: * Dashed lines are SKB results, solid lines are AMBER. SKB results have been adjusted by a factor of 0.175 to take account of the different LDF values used. This factor is simply the ratio of the peak values calculated for the Q1 pathway by AMBER and SKB.

Figure 5: Comparison of Releases of Key Radionuclides, AMBER Reference Case and SKB, All Near-Field Pathways

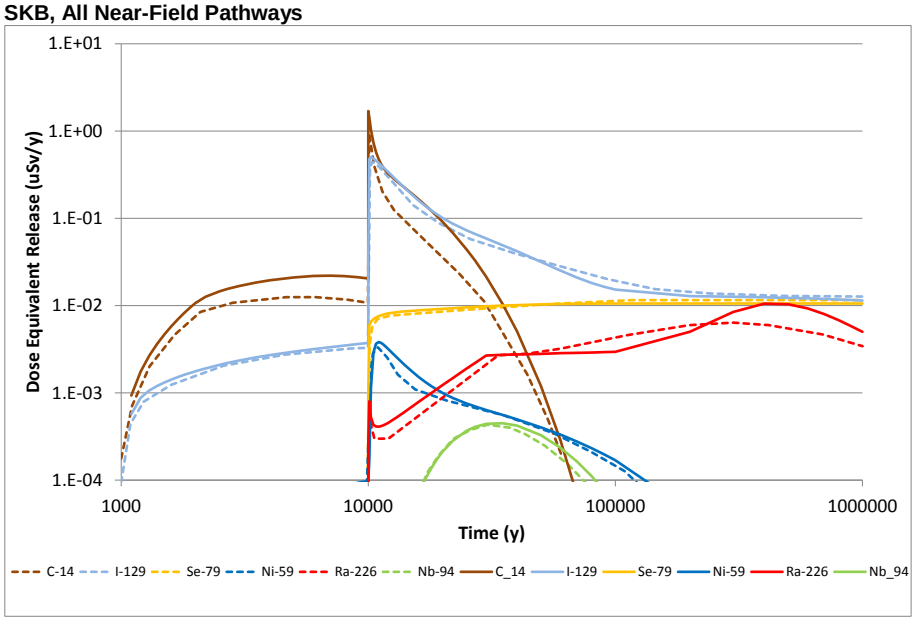

Note: * Dashed lines are SKB results, solid lines are AMBER.

For C-14, the release calculated by SKB is slightly lower than that calculated with AMBER. This difference is likely to be associated with the detailed representation of the diffusion through the buffer, suggesting that there is less diffusion vertically in the AMBER model than calculated by SKB. The results for Se-79, Nb-94 and I-129 agree well. For Ra-226 the AMBER model shows some differences in the structure of the curve in the period after 50,000 y. Determining the basis for this difference is complicated due to the influence of its long-lived parents U-234 and

Th-230. Nevertheless, the peak values are in reasonable accord with SKB's results. Finally, whilst the initial peak associated with Ni-59 matches closely the SKB results, the subsequent behaviour is different, with SKB calculating a more rapid decline in the releases. The reason for this difference has not been fully determined, but could be a result of corrosion releases and solubility limitation. Specifically, it is noted that the majority (96%) of Ni-59 is released by corrosion, which – using reference assumptions – occurs on a timeframe of 1,000 – 2,000 y, and the solubility limit is reached in the period up to 10,000 y. In AMBER, corrosion releases are not constrained by solubility and are assumed to immediately precipitate in the canister void if the solubility limit is reached. If solubility were to constrain the corrosion process, a greater proportion of the Ni-59 would be held up in the cladding until after 10,000 y, when the hole grows to a large size, and then be released. A further area of uncertainty is the treatment by SKB of the effect of stable Ni on solubility – at present this is not included in the AMBER calculations, as SKB only discuss the role of stable elements in relation to Ra and Ag (see Section F.5 of SKB (2010a)).

The calculation case has also been evaluated in both deterministic and probabilistic modes to explore the significance of parameter distributions in the overall evaluation of the near-field system performance. Case P5 (shown in Figure 5) includes median values for all parameter distributions and is calculated deterministically. Case P6 includes PDFs for all uncertain parameters, as specified by SKB (2010b) but does not sample geosphere parameters such as the groundwater flow properties, equivalent flow rates and solubility limits (sorption coefficients are, however, sampled). Figure 6 presents a comparison of the results gained for the probabilistic case with those for the deterministic case.

Figure 6: Summary of the Results of Probabilistic Calculations for the Near-field with Deterministic (Median) Geosphere Properties

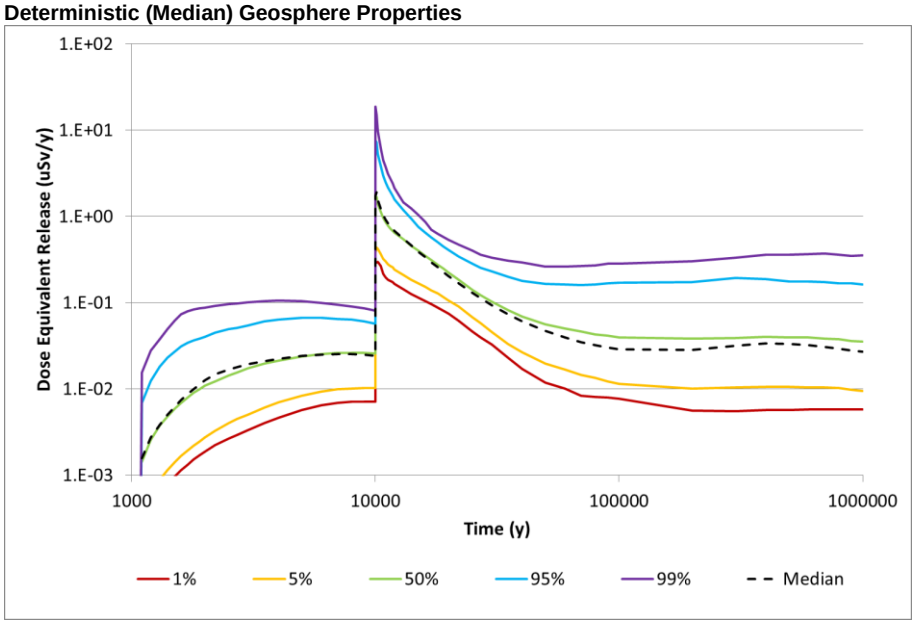

It can be seen that the median deterministic case matches very closely with the median of the probabilistic calculations (even though only 100 realisations were evaluated). Prior to 10,000 y the difference between the 1st and 99th percentile results is about a factor of ten, as a result of the range of release fractions and corrosion timescales. At longer times (in excess of 400,000 y) this increases to more than a factor of 50. The most significant parameter is the Fuel Conversion Rate,

which determines the rate of release of key radionuclides including I-129. A scatter graph (Figure 7) shows that this has a very strong influence on the calculated dose at 1,000,000 y, with a range of results from 7 10^{-3} to 0.1 µSv/y. The feature occurring at around 7 10^{-8} /y is related to the point at which the fuel conversion rate becomes sufficiently low to mean that Se-79 is no longer solubility limited at long timescales.

Figure 7: Scatter Graph Showing the Influence of Fuel Conversion Rate on the Calculated Dose Equivalent Near-Field Release at 1,000,000 y

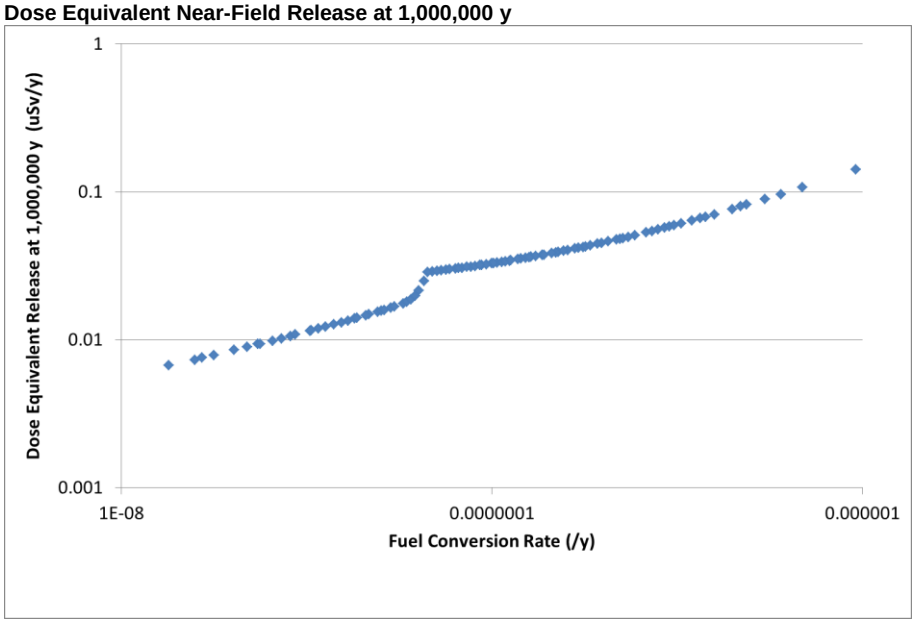

Comparing deterministic and probabilistic results for individual radionuclides shows that there is little difference for most radionuclides. Figure 8 compares the deterministic case, which is based on median values for parameter distributions, with the mean results for around 1000 realisations of a probabilistic calculation (all the realisations that ultimately lead to a release). For most radionuclides, differences are small, less than a factor of two at the greatest, and reflect the influence of some non-symmetrical and logarithmic distributions in which the median and mean can be significantly different. Notable differences are, however, observed for radionuclides such as Se-79, Nb-94 and Ra-226. These occur where the rate of release is dependent on parameters that have a large range in value (e.g. Fuel Conversion Rate) and for which the mean value is significantly greater than the median.

Figure 8: Comparison of Deterministic Median with Probabilistic Mean Results for the Release of Key Radionuclides from the Near-field

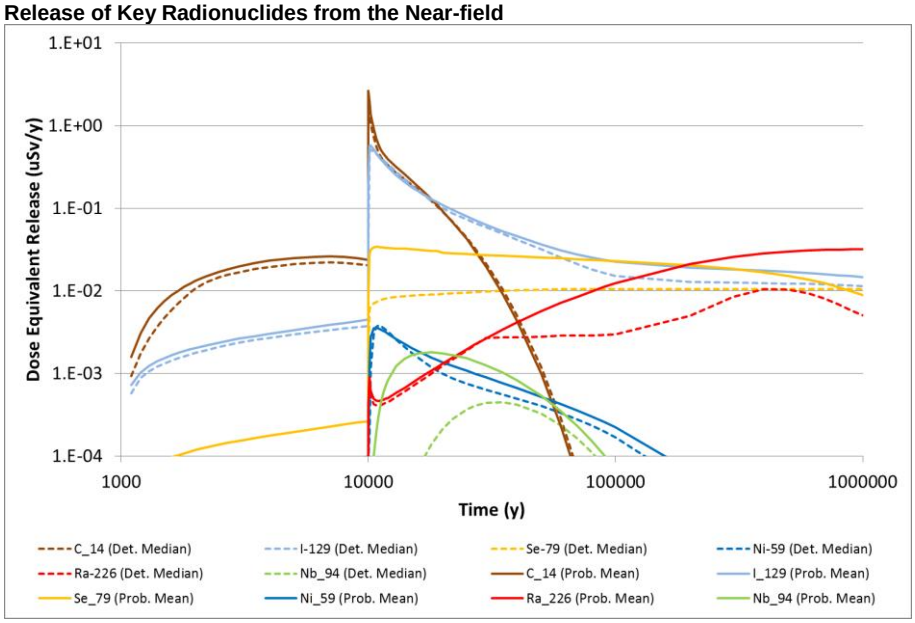

4.2.2. Far-Field

Calculation Cases

Limited information is provided by SKB concerning the specific approach to representing contaminant migration in the far-field. For example, SKB (2010a) do not discuss whether sorption on fracture surfaces is represented. Another important factor is the maximum penetration depth for diffusion. SKB select a value of 12.5 m, half of the average fracture spacing. This is a large matrix diffusion depth and can potentially introduce numerical issues, in particular with compartment modelling approaches, due to the relative size of compartments representing the fracture and the rock adjacent to it.

Nevertheless, the basic approach – a one dimensional advection/dispersion model with diffusion perpendicular to the direction of flow – is well understood. Compartment modelling approaches for the main processes are well established. One of the key considerations in relation to dispersion and diffusion is the required level of discretisation. This is important because the more discretisation that is applied, the greater the number of compartments and transfers, which in turn increases runtime. The focus of the model prototyping is therefore on the extent of discretisation required both in respect of advective-dispersive transport and diffusion.

P6 and P7: Alternative Discretisation of Advective Pathway

Dispersion is normally dealt with by dividing the transport pathway into a number of compartments equal to half of the ratio of the dispersion length to the total length (a value sometimes referred to as the Peclet number). SKB (2010b) (Table 6-85) specify a Peclet number of 10 implying the need for at least 5 compartments to represent advection-dispersion. However, if the overall dynamics of contaminant

transport in the model are dominantly controlled by the near-field release, fewer compartments could potentially be used in to represent the far-field.

The reference case adopts 5 compartments to represent the pathway. Two alternate cases have been considered:

- No discretisation of the pathway (a single compartment to represent the whole pathway);
- Discretisation of the advective pathway into 3 compartments.

These cases will indicate the sensitivity of the system to the representation of dispersion in the fracture pathway.

P8 and P9: Alternative Discretisation of Diffusive Pathway
Diffusion also requires a certain degree of discretisation in order to adequately represent the process. As discussed previously, the accuracy (compared with an analytical solution) is equal to $1/n^2$ where n is the number of compartments used to discretise the region in which diffusion takes place. In order to gain an insight into the most appropriate degree of discretisation, the following cases have been considered:

- Discretisation of the rock matrix into a single matrix compartment; and
- Discretisation of the rock matrix into 3 compartments.

As with the advective pathway, the significance of the matrix diffusion process is dependent on a number of factors including the characteristics of the release and the advective transport velocity in the fracture.

Comparison with SKB Results

The reference case and four different approaches to the discretisation of the far-field are compared with the results obtained by SKB (2010a) for a growing pinhole in a single canister (Figure 6-14 (SKB, 2010a)). All radionuclides were considered, but the focus was on the dominant Q1 pathway only. The results, presented in Figure 9, illustrate that the model is sensitive to the representation of matrix diffusion. Omitting the rock matrix diffusion pathway, or representing it with only a single matrix compartment, results in significantly greater releases (a factor of 5) due to less dispersion over time of the releases from the near-field. This is illustrated by the much sharper peak shortly after 10,000 y.

By comparison, coarser discretisation of the advective component of the pathway, even adopting only a single compartment to represent the whole pathway, makes little difference to the calculated results (peak dose equivalent release of 0.31 µSv/y compared with 0.24 µSv/y for the reference case in which 5 compartments are used to represent the advective transport pathway). This observation indicates that matrix diffusion is the dominant process for this case and that less discretisation of the far-field fracture pathway may be acceptable to enable more rapid calculations.
When the reference results are compared with SKB's model results some further differences can be noted. Although the form of the curve is very similar to that calculated by SKB the peak value calculated in AMBER is lower, whereas the long-term dose equivalent releases (beyond about 30,000 y) are higher. Investigations showed that this is mainly due to the use of distributed LDF values in the AMBER calculations compared with the basic LDF values used by SKB (2010). If the AMBER model is used with the basic LDFs for C-14, I-129 and Se-79 then the peak value (dominated by C-14) is within a factor of 2 of the SKB results (less for I-129),

and the longer term results are within about 50% of the SKB results. A comparison of these key radionuclides is shown in Figure 10.

Figure 9: Comparison of Various Schemes for the Discretisation of the Q1 Geosphere Pathway with SKB Results

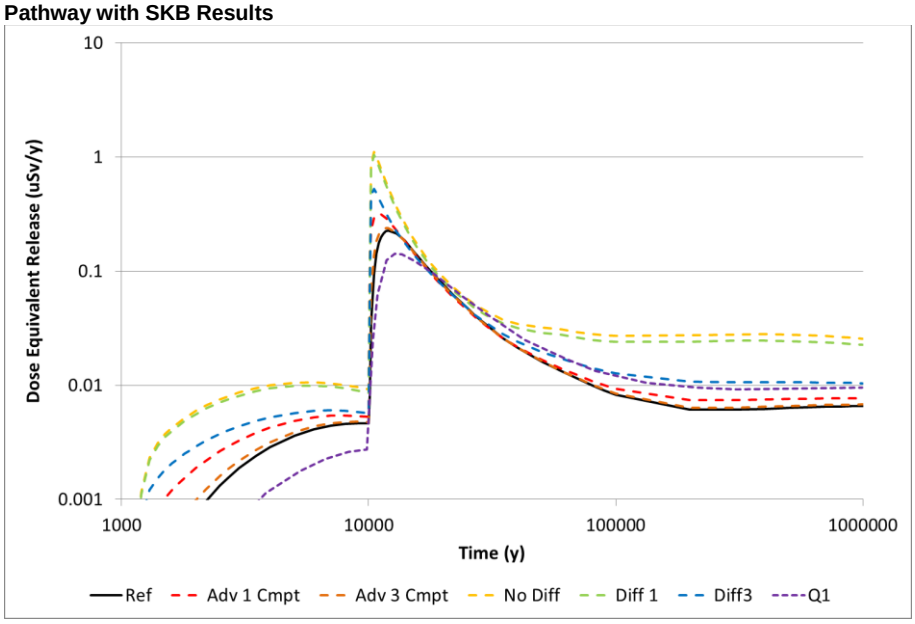

Figure 10: Comparison of the Reference AMBER Results with SKB's Results for the Growing Pinhole Case, Deterministic Calculations and Basic LDF Values

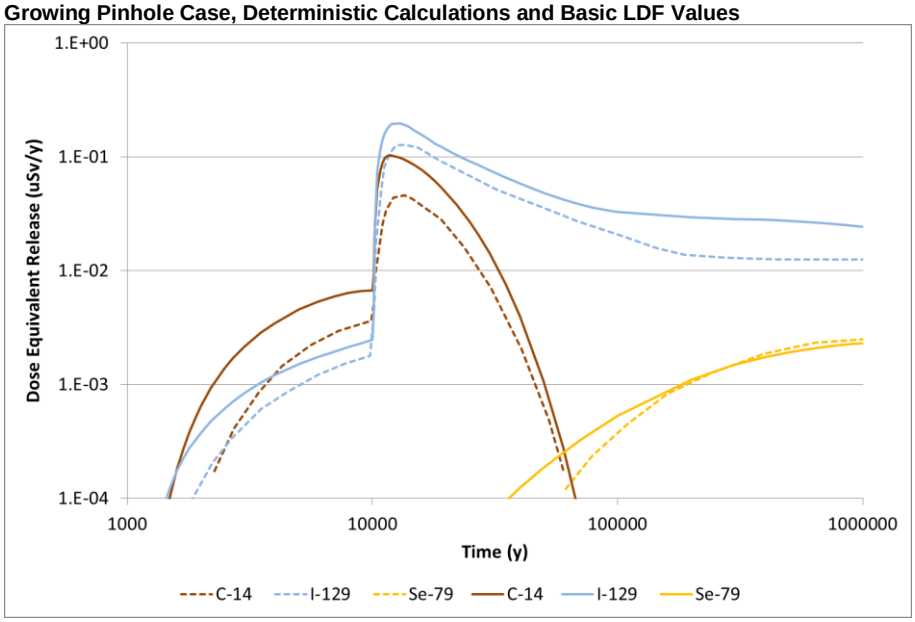

Note: * Dashed lines are SKB results, solid lines are AMBER.

When considering probabilistic calculations it is necessary to include parameter distributions derived from supporting codes (specifically, the ConnectFlow and related analyses) because geosphere transport properties are mainly derived from such codes. This includes aspects such as the contaminant travel time.

The distribution of calculated dose equivalent releases, shown in Figure 11, illustrates the considerable influence of the sampled geosphere properties on the calculated dose equivalent releases. As previously, the deterministic result, calculated with median values, is similar in value to the 50%ile of the probabilistic evaluation. This is the case for individual radionuclides as well as the total dose equivalent release, as illustrated in Figure 12, with the exception of Se-79. This radionuclide is strongly influenced by the near-field release rate and sorption in the rock matrix. Wide ranges are specified for these parameters, and the mean of values is significantly higher than the median. As a consequence, the mean tends towards a more rapid and early release from the far-field.

Figure 11: Summary of the Results of Probabilistic Calculations for the Far-field with Deterministic (Median) Groundwater Flow Properties

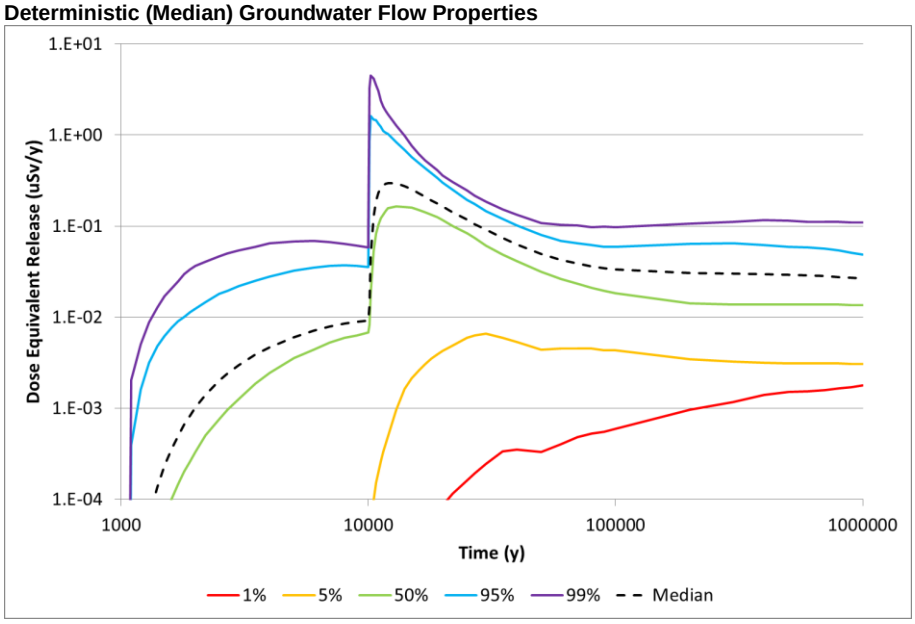

Figure 12: Comparison of Deterministic Median with Probabilistic Mean Results for the Release of Key Radionuclides from the Far-field

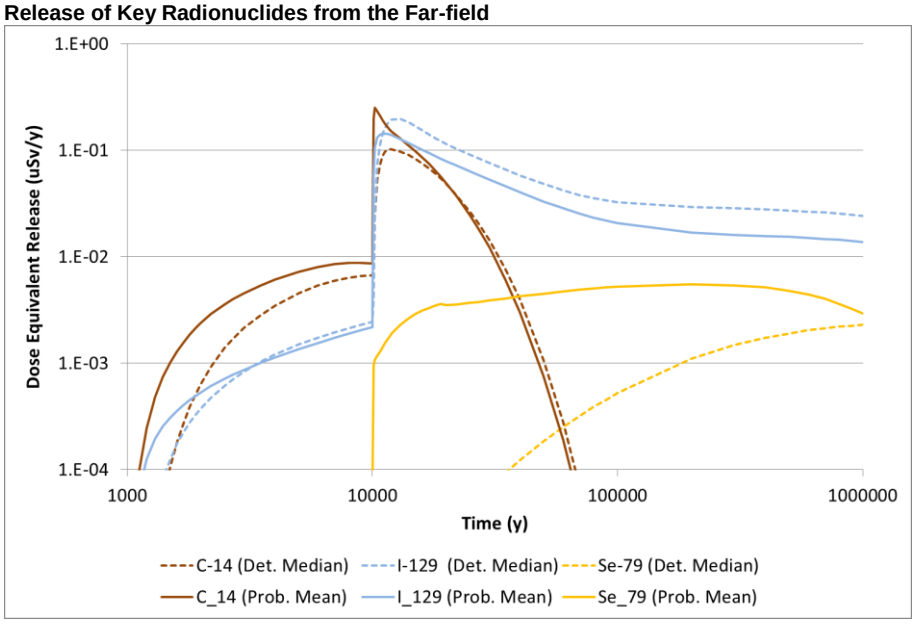

The similarity of the trends with the near-field results suggests that the dominant factor in the variation in the results at long timescales remains the Fuel Conversion Rate. Figure 13 demonstrates that this is the case, with a near linear response between the Fuel Conversion Rate and the calculated dose equivalent far-field release at 1,000,000 y. The relationship found for the far-field is very similar to that for the near-field (Figure 7) except that it does not include the feature seen at a Fuel Conversion Rate of about 7 10^{-8} y^{-1} in Figure 7. This feature corresponds to the point below which the Fuel Conversion Rate is more limiting to Se-79 release than its elemental solubility. It is evident in Figure 7 because Se-79 represents about 50% of the dose equivalent release from the near-field at 1,000,000 y. However, in the geosphere elemental sorption means that Se-79 contributes far less to the total dose equivalent release at 1,000,000 y (only about 10%, see Figure 12). As a consequence of the dominance of I-129, which is not affected by solubility, this feature is not sufficiently significant to be noted in Figure 13.

Figure 13: Scatter Graph Showing the Influence of Fuel Conversion Rate on the Calculated Dose Equivalent Far-Field Release at 1,000,000 y

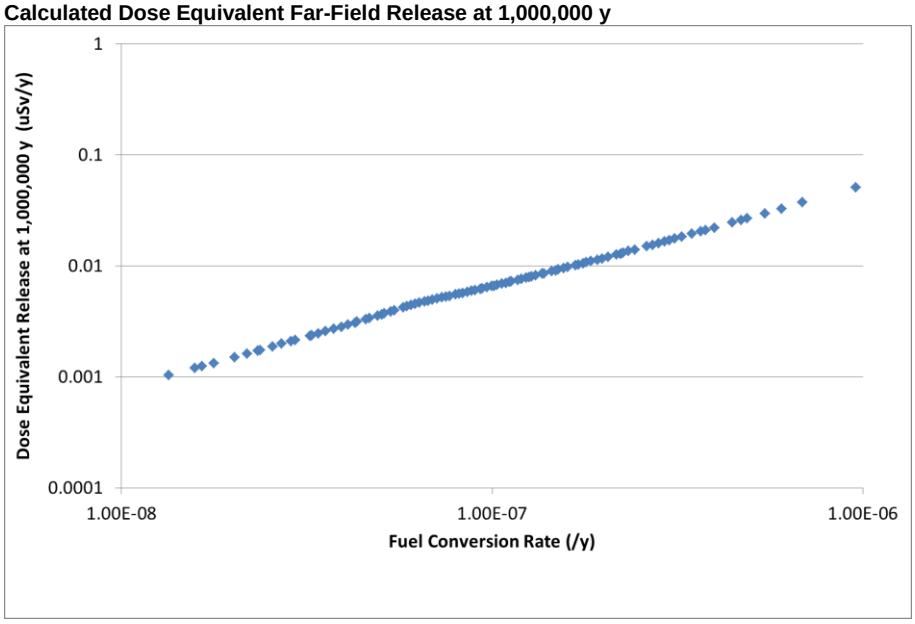

5. Results

AMBER calculations, using the model developed as a result of the prototyping stage described in Section 4, were compared with the results presented by SKB in the radionuclide transport report, Section 6.5 (SKB, 2010a). SKB's key results are the dose equivalent releases from the near-field, i.e. the radionuclide flux multiplied by the appropriate LDF. SKB (2010a) does not provide supplementary information for these cases, such as concentrations in intermediate media (e.g. different parts of the buffer, backfill and rock matrix), which limits the extent to which any differences in results can be explored in detail. Far-field dose equivalent releases calculated by AMBER were also compared with SKB (2010a). In broad terms there was less emphasis on this aspect, as the focus of this study was to examine SKB's calculations to analyse barrier performance.

5.1. Case A

5.1.1. Near-Field

Case A examines the role of the buffer in deposition holes. It is based on the "Initial Advection" case presented as part of SKB's alternative calculation cases (Section 4.5 of SKB (2010a)) which explores the consequences of canister corrosion due to absence of sufficient buffer to fill a deposition hole. Case A extends this to all deposition holes, thereby seeking to highlight the role of the buffer component of the disposal system.

This situation was represented by introducing a water-filled connection between the canister and the Q1 pathway. In AMBER model, the case has been represented by changing the material type of all "Block 3" compartments (connecting the Canister to the Q1 fracture) to be water rather than buffer. Transport calculations through these compartments therefore adopted the properties of water, and thus when the defect occurs the contaminants were rapidly released into the water filled section of the buffer. Solubility limitation was not applied in Block 3 except for uranium and thorium, consistent with the assumptions made by SKB in the description of the calculation case in Section 4.1.2 and 4.5.9 of SKB (2010a).

The time at which canisters fail is determined by the corrosion rate and groundwater conditions. SKB's supporting codes have determined the failure times of canisters, and concluded that a total of 84 of the 6916 deposition holes could fail within 1,000,000 y, with a likelihood of 0.17 canisters failing. SKB note that for Case A and Case A* calculations only the Q1 pathway was considered because it dominates the radionuclide releases (see Section 6.5 of SKB (2010a). The Q2 and Q3 pathways were therefore not modelled in AMBER for this case.

SKB presents results for a deterministic calculation that considers missing buffer in a single deposition hole in Section 4.5.9 of SKB (2010a). This calculation assumes the failure of a canister at the earliest of the calculated times, shortly after 44,000 y and uses deposition-hole specific geosphere properties. It was not possible to recreate the calculation with AMBER because the corresponding geosphere

properties could not be identified in the available data files. Scoping calculations were undertaken using median geosphere properties but these did not show any obvious correspondence with the results presented by SKB in Figures 4-28 and 4-29 of SKB (2010a), due to the variability in sampled properties and their influence on the model response.

A comparison could, however, be made with SKB's probabilistic analysis of the missing buffer case. The full set of 84 failure times calculated by SKB was used in a probabilistic AMBER calculation case, along with other uncertain parameters that were also sampled. The results have been presented in Figure 14, which is compared with Figure 4-30 from SKB (2010a). Here, the AMBER results represent the mean of the calculated dose equivalent releases for the 84 realisations in which corrosion is calculated to occur by SKB, multiplied by the probability of a canister failing of 0.17.

Figure 14: Comparison of Dose Equivalent Releases from the Near-Field Calculated by AMBER and SKB* – Case A (Mean of 84 Failed Canisters)

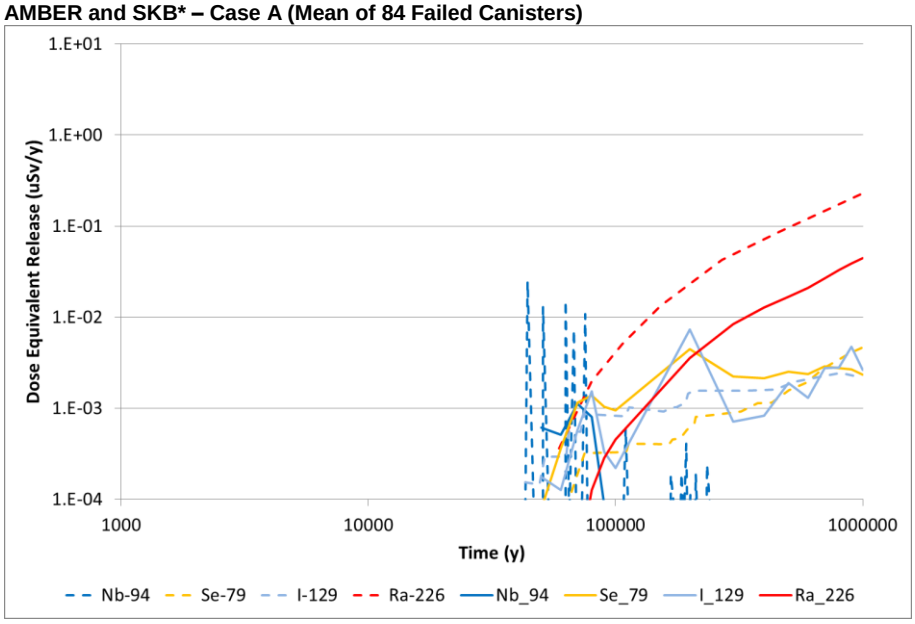

Note: *Dashed lines indicate SKB results, solid lines indicate AMBER results

The reason that the spiky releases of Nb-94 were not seen in the AMBER results is that AMBER requires specific output times to be defined prior to the calculations. To accurately capture these rapid releases of contaminants from the near-field, a very large number of output times would be required and it was not been possible to adequately specify these times in AMBER in a probabilistic calculation case. The AMBER results nevertheless showed this radionuclide to be released at approximately the same time as SKB calculations. Although the AMBER output times did not capture the very sharp peaks, the calculated releases can be seen to be of a similar scale.

For the other radionuclides, the form of the releases, as a function of time, was very similar for the key radionuclides - Se-79, I-129 and Ra-226. The magnitude of the dose equivalent releases of was also similar to the SKB results in Figure 4-30 of SKB (2010a). The results for Se-79 and I-129 matched SKB results closely at 1,000,000 y, but there were differences at earlier times. Notably, releases of Se-79 were typically greater than SKB calculations, by a factor of about 5. The results for Ra-226 were about a factor of 5 times lower.

The main difference between Ra-226 and the other radionuclides is that it is a daughter product of longer-lived, much less mobile, radionuclides, whereas I-129 and Se-79 are long-lived mobile radionuclides that are not part of a decay chain. The issue of solubility limitation was explored, and examination of the detailed results showed that Ra-226 and its parent radionuclides were solubility limited immediately upon release.

If the individual sample results are examined it can be seen that SKB's mean probabilistic result lies well within the envelope of AMBER results (see Figure 15), although tending towards the realisations that lead to higher dose equivalent releases. This figure also illustrates that there is a considerable range in the maximum dose equivalent release even when the time the canister is assumed fail is similar. For example, there can be seen to be a range in the dose equivalent release of about a factor of 50 for those canisters that fail before 100,000 y. Further examination of the results shows that the main factor responsible for the spread in results was the sampled Fuel Conversion Rate. Figure 16 shows as clear dependency of the dose equivalent release of Ra-226 on this parameter. This is because the rate of release of this radionuclide from the fuel is controlled by the Fuel Conversion Rate.

Figure 15: Comparison of SKB's Mean Dose Equivalent Release of Ra-226 with Individual Sample Results Calculated by AMBER

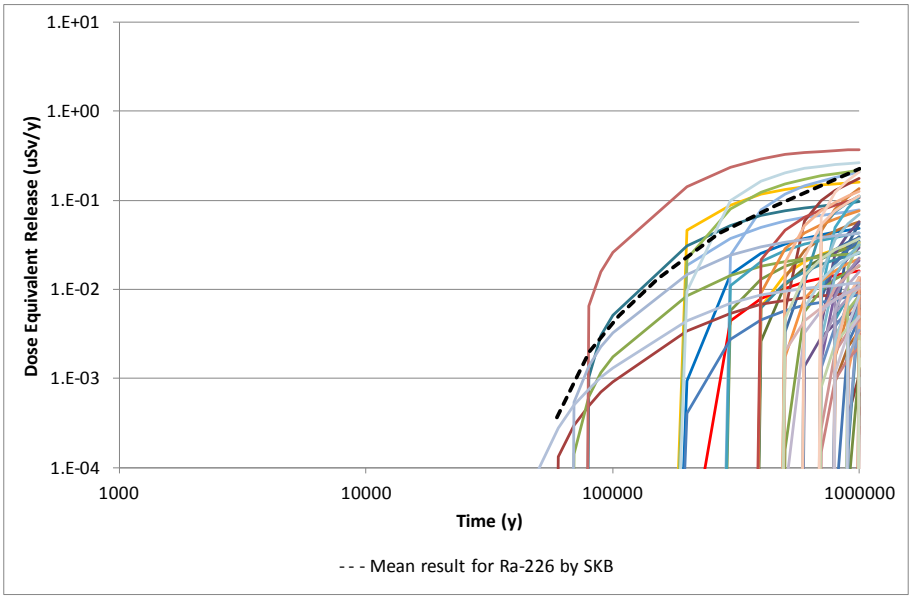

Given that the rate of release of Ra-226 is strongly dependent on a sampled parameter, and there are relatively few samples in this calculation (84) it is probable that differences between the SKB results and the AMBER results are a consequence of the specific sampled values used in the calculation. Differences in the sampled values of, say, Fuel Conversion Rate that were used for the calculation of the realisations involving corrosion before 100,000 y would have a substantial effect on the calculated mean release. Although the sampled corrosion times used in AMBER were the same as used by SKB (as the values were specified in a specific data file) other parameters, such as the Fuel Conversion Rate, were sampled independently by AMBER. Furthermore, none were correlated in the AMBER calculations.

Figure 16: Variation in Dose Equivalent Release of Ra-226 from the Near-field, Calculated by AMBER, with the Fuel Conversion Rate

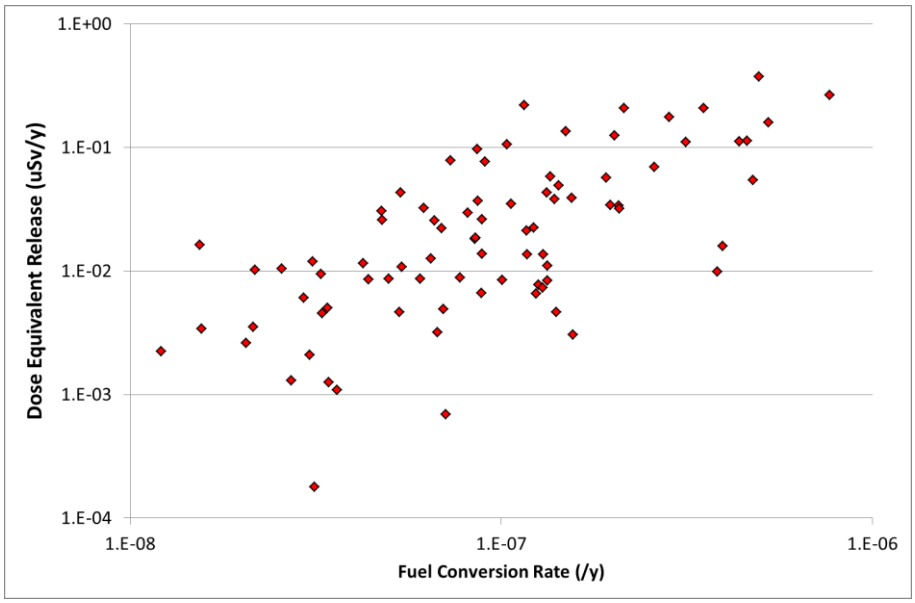

5.1.2. Far-Field

The dose equivalent releases from the far-field calculated by the AMBER model are shown in Figure 17 and compared with results from Figure 4-31 of SKB (2010a). SKB indicate in Section 6.5 (SKB, 2010a) that these results are representative of the calculated releases for Case A.

Figure 17: Comparison of Dose Equivalent Releases from the Far-Field Calculated by AMBER and SKB* – Case A

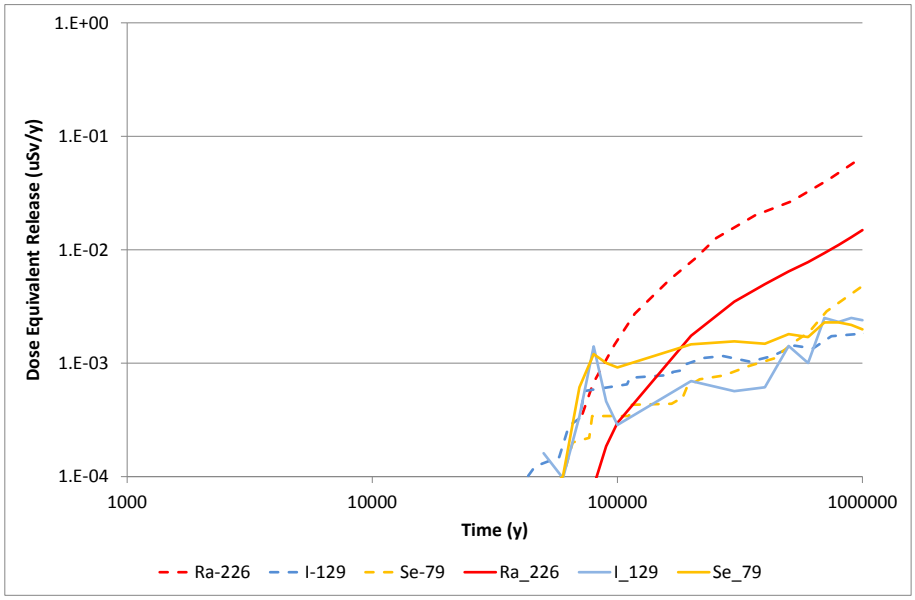

Note: *Dashed lines indicate SKB results, solid lines indicate AMBER results

The general trend was the same as found in the comparison of the near-field results. Because no geosphere sorption was modelled in this case, the relative importance of the radionuclides was unchanged compared with the near-field releases. The profile in time of the releases of each radionuclide was also similar to that calculated by SKB, which indicates that the contaminant transport processes were modelled in the same way. Furthermore, the relative significance of each radionuclide was the same as observed for the near-field releases of Se-79, I-129 and Ra-226.

In broad terms, the results indicated that the geosphere does not have a significant role as a barrier to radionuclide releases of contaminants when sorption is not modelled. Figure 18 shows that contaminants only diffused to a significant degree into the first three rock matrix compartments in the AMBER Model (which represent a thickness of about 45 cm). Because of the low porosity of the rock (0.18%) and the limited diffusion depth the majority of the contaminants were present in the fracture, where the travel time (a median value of 180 y) was rapid compared with the timeframe of the releases.

Figure 18: Calculated Pore-fluid Concentrations of Ra-226 in the Far-field Compartments Associated with the Q1 Pathway Modelled by AMBER for Case A

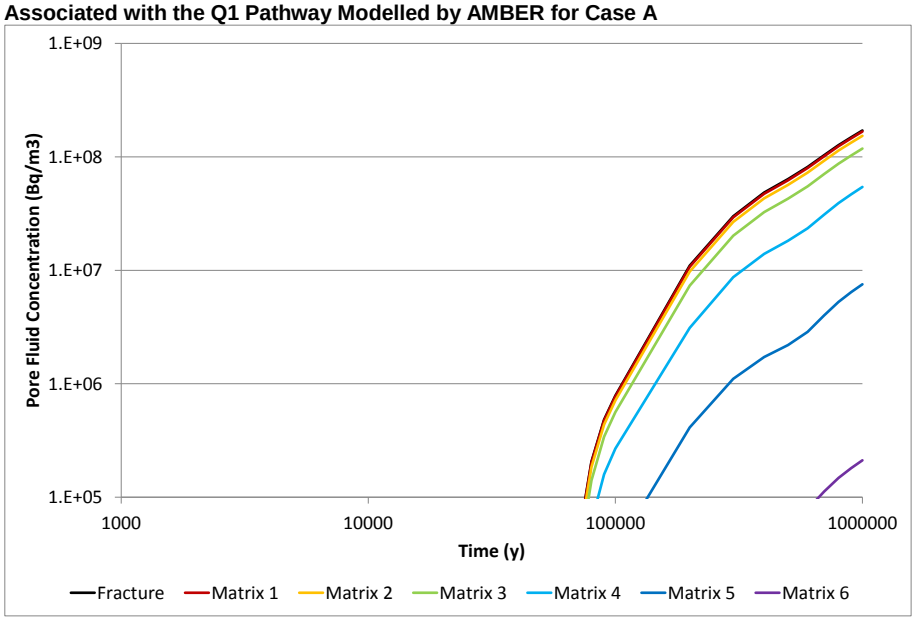

The rate of release of contaminants is dependent on the amount retained in the rock mass. This in turn is determined by the porosity, effective diffusion coefficient, and sorption coefficient.

Matrix porosity was not assigned a distribution in SKB's calculations, but the rate of release from the far field can be assumed to be relatively insensitive to the parameter. This is because the volume of contaminated pore fluid in the matrix is substantially lower than the volume in the fracture. Using the median fracture thickness, and assuming equilibrium concentrations in a 45 cm thickness of rock (based on Figure 18), a porosity of 0.0018 implies that 98% of the contaminated water is in the fracture and only 2% in the rock matrix.

The depth of diffusion is controlled by the effective diffusion coefficient, which was sampled by SKB. Significantly more rapid diffusion through the rock does have the possibility of reducing the amount of contaminants in the pore fluid, as a greater proportion of the contaminants could be distributed in the rock mass. For the rock characteristics defined by SKB, however, the parameter did not have a significant effect on the rate of release from the far-field. This is shown by Figure 19, which shows that there was no obvious dependency of rate of release for key radionuclides on the effective diffusion coefficient value.

Figure 19: Variation in Dose Equivalent Release from the Far-field, Calculated by AMBER, with the Effective Diffusion Rate in the Rock Matrix

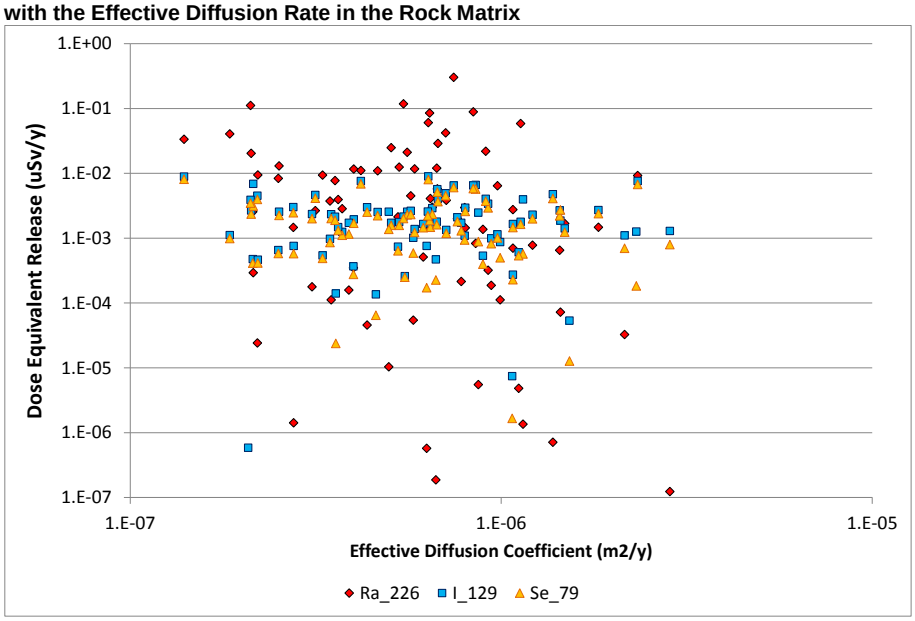

Finally, it is noted that the sorption coefficient will reduce the amount of contaminants released from the far-field by increasing the capacity for the retention of sorbed radionuclides in the rock. I-129 is unsorbed, but the influence of sorption on Se-79 and I-129 can be seen in Figure 20. When sorption is modelled the Ra-226 releases were reduced by a factor of about 30 and the Se-79 releases by a factor of approximately 3.

Figure 20: Comparison of the Dose Equivalent Release Rates Calculated by AMBER when Sorption is Represented or Neglected

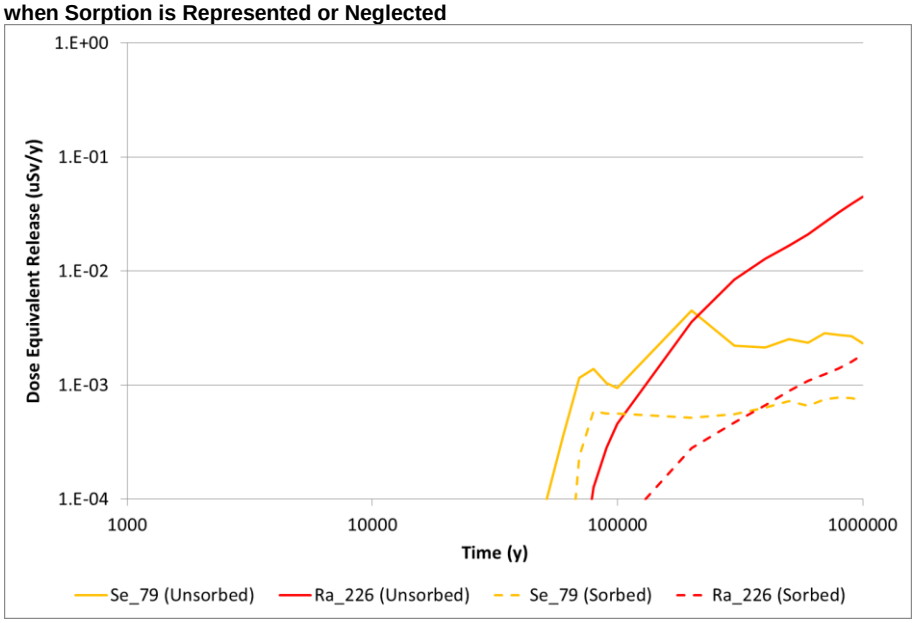

5.2. Case B

5.2.1. Near-Field

A "growing pinhole" in single canister is presented by SKB as a main calculation case in its analysis of barrier functions. The same conceptual model has been used in "Case B" that is evaluated here, but extended to apply a growing pinhole to all deposition holes. Case B was used to prototype the AMBER model, as discussed in Section 4 of this report, where aspects of the performance of the model have already been discussed. This section presents a comparison of the results gained with the final AMBER model and SKB's main results. The main point of comparison was the results calculated for the single canister "growing pinhole" case (discussed in Section 6.3 of SKB (2010a)) from which Case B was derived, because SKB do not present detailed results for Case B.

Figure 21 presents the dose equivalent releases from the near-field calculated by the deterministic AMBER case and compares them with SKB's results from Figure 6-11 (SKB, 2010a). The broad conclusion that can be drawn was that the AMBER model gave good agreement with the SKB calculations. Some minor differences were seen for C-14 and Ra-226 at certain times, at which the AMBER results differed by up to a factor of five. This typically corresponded to a larger release calculated by AMBER, as can be seen from Figure 21.

Consideration of the AMBER results for different pathways suggested the difference in C-14 releases could be related to the Q2 and Q3 pathways. This is indicated in Figure 4, which can be compared with SKB's deterministic results in Figure 6-12 of SKB (2010a) (noting that this figure was calculated with the basic LDF values which resulted in dose equivalent releases about an order of magnitude greater than those calculated from the distributed LDF values used in the AMBER calculations).

Figure 21: Comparison of Dose Equivalent Releases from the Near-Field Calculated by AMBER and SKB – Case B (Single Canister Only, Deterministic Case)

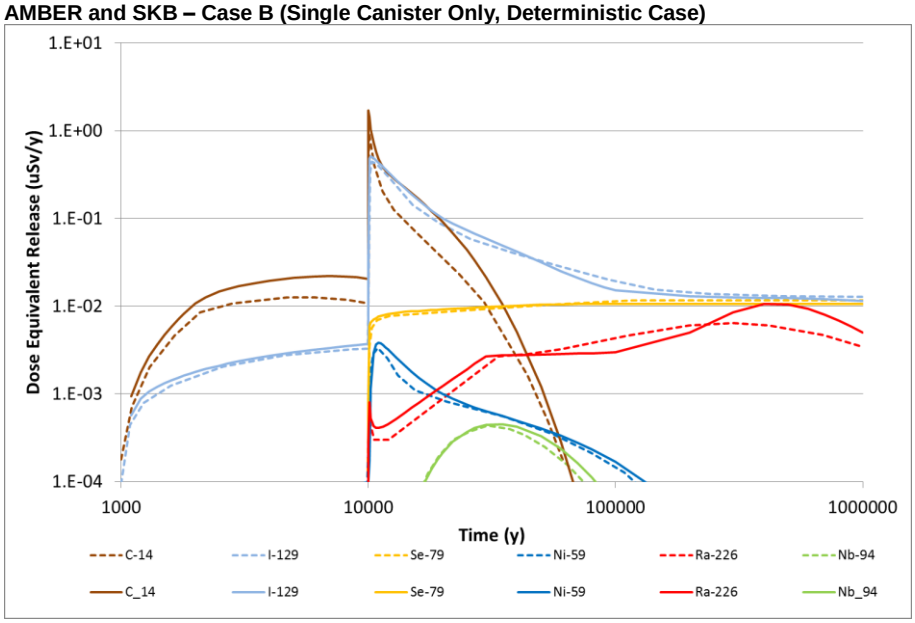

Note: * Dashed lines are SKB results, solid lines are AMBER results.

The reasons for this difference were unclear, because the near-field model defined by SKB in Appendix G of SKB (2010a) was implemented directly in AMBER, and key parameters such as the equivalent flow rate were taken directly from SKB data files. Nevertheless, the broad conclusion that can be drawn was that the deterministic AMBER model gave good agreement with the SKB calculations.

A comparison of the mean AMBER and SKB results (from Table 6-15 of SKB (2010a)) for probabilistic calculations of Case B has been shown in Figure 22. The SKB results were calculated from 6916 realisations, whereas only a subset of realisations that give rise to a release (1175 out of 6916) were included in the AMBER calculation. The results were nevertheless similar, although there was less agreement than found for the deterministic case. Most notably, Ra-226 releases were substantially lower than calculated by SKB, as found with Case A. It can also be noted that for radionuclides such as I-129 and Se-79 the AMBER releases were significantly lower at longer timescales.

The probabilistic AMBER model was used to explore the key parameters that control the releases of radionuclides. For example, the Fuel Conversion Rate was a key factor for the long-term doses associated with I-129, but had a significantly weaker influence on other contaminants (see Figure 23). For radionuclides that were solubility limited, such as isotopes of uranium and thorium, the solubility was a key parameter that determined the rate of release over long timeframes.

The peak dose equivalent release (occurring at around 10,000 y) was strongly influenced by the equivalent flow rate from the near-field for most radionuclides, as illustrated in Figure 24. In this figure, it can be sent to exhibit a particularly strong influence on C-14 releases. Noting the suggestion from other results that diffusion into the buffer was an important factor for the longer-term releases of contaminants, the relationship between the effective diffusion coefficient and the dose equivalent release was also explored for both anions and cations. As can be seen in Figure 25, no strong dependency was observed.

Figure 22: Comparison of Mean Dose Equivalent Releases from the Near-Field Calculated by AMBER and SKB – Case B (Single Canister Only, Probabilistic Case)

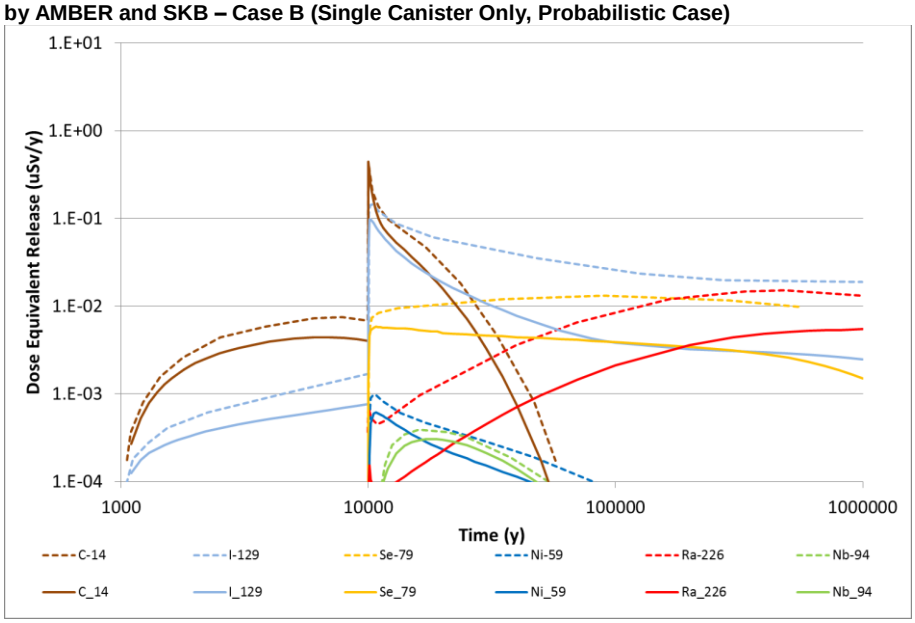

Note: *Dashed lines indicate SKB results, solid lines indicate AMBER results

Figure 23: Influence of Fuel Conversion Rate on the Dose Equivalent Release Associated with Various Radionuclides at 1,000,000 y

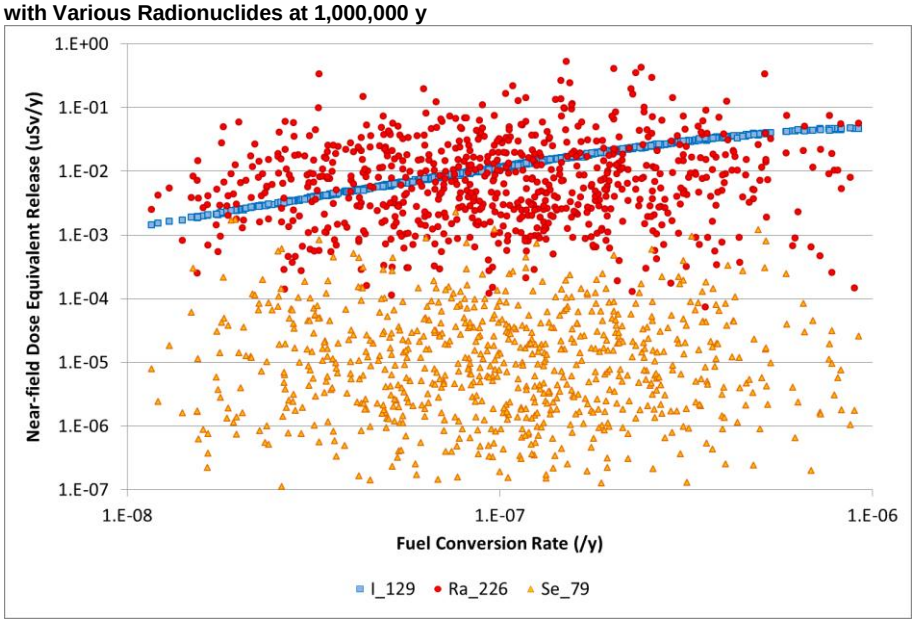

Despite the apparent differences for the probabilistic calculations, the AMBER calculations can be interpreted as showing that the SKB results provide a suitable representation of the performance of the disposal system in terms of Case B. The key aspects of the results, including the sharp increase in releases when the pinhole increases in size, and the long-term releases from Se-79, I-129 and Ra-226, are confirmed. Where differences occur, AMBER results tend towards lower calculated releases than SKB.

Figure 24: Influence of Equivalent Flow Rate on the Dose Equivalent Release Associated with Various Radionuclides at 10,000 y

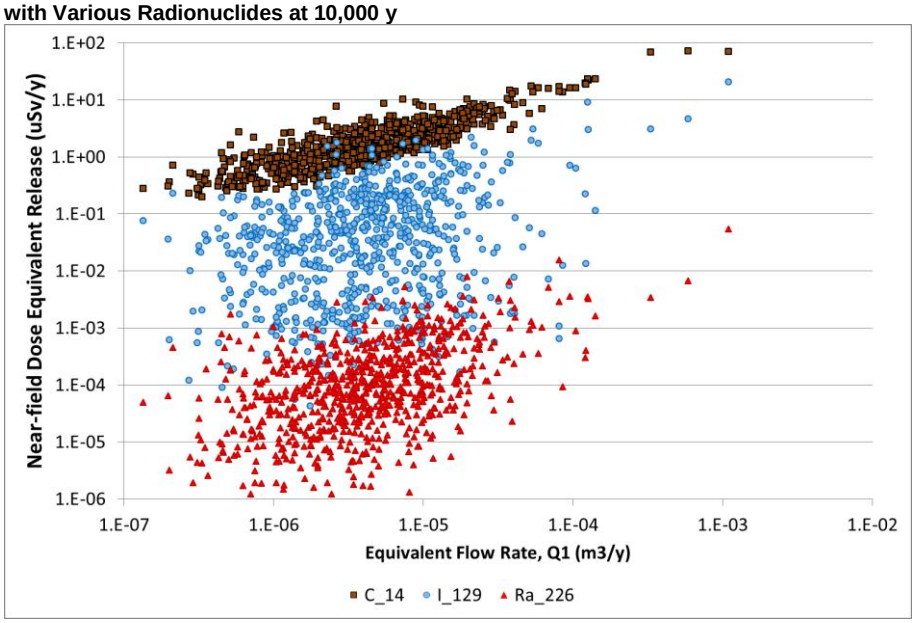

Figure 25: Influence of Effective Diffusion Coefficient on the Dose Equivalent Release of Selected Cations at 100,000 y

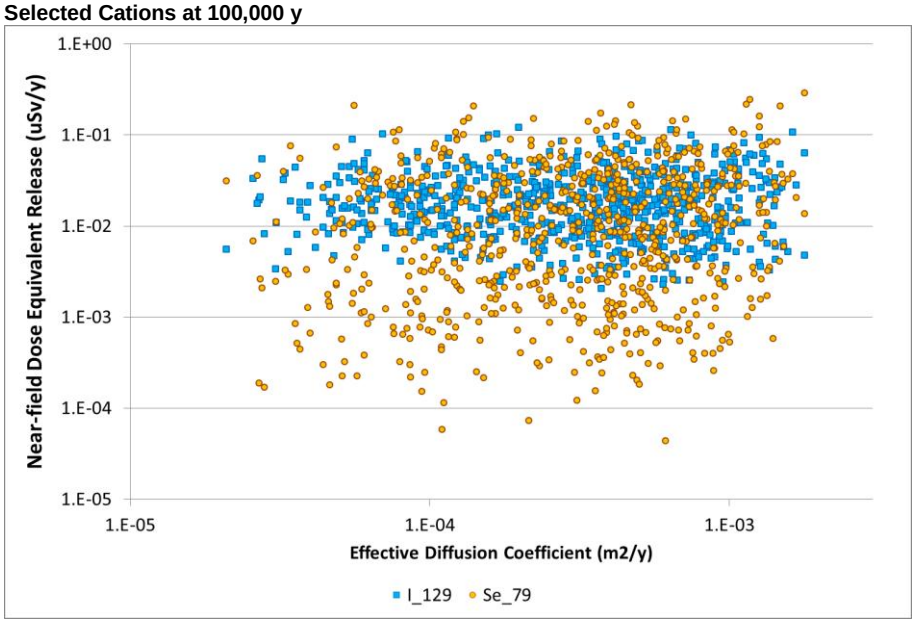

5.2.2. Far-Field

The calculated dose-equivalent releases from the geosphere are presented in Figure 26 and compared with the results calculated by SKB. The basis for comparison was again the single-canister deterministic case (Figure 6-13 of SKB (2010a)) as SKB do not present detailed results for Case B in Section 6.5 of SKB (2010a). The differences associated with the near-field releases of C-14 in the period up to 10,000 y, and shortly after, were also evident in the far-field results. The calculated releases for Se-79 matched well, but, in contrast to the near-field results, the C-14 and I-129

AMBER results were about a factor of five greater than those calculated by SKB. The far-field results therefore exhibited a different trend from those calculated for the near-field, although the broad shape of the curves describing the releases as a function of time is similar to that calculated by SKB.

Figure 26: Comparison of Dose Equivalent Releases from the Far-Field Calculated by AMBER and SKB – Case B (Single Canister Deterministic Case)

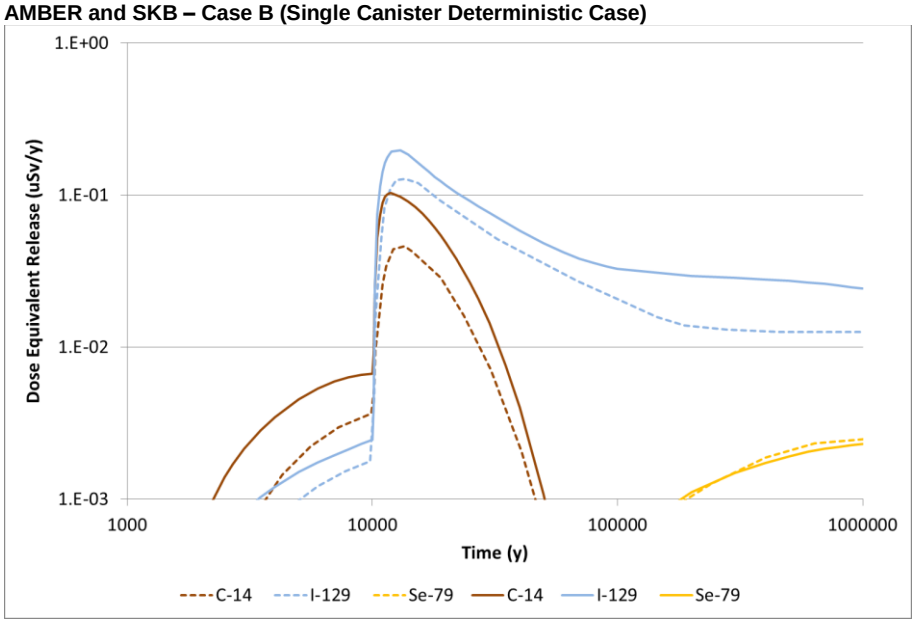

Note: * Dashed lines are SKB results, solid lines are AMBER results.

Examining each pathway in turn indicated that the differences noted for the near-field releases via the Q2 and Q3 pathways were carried through to the far-field results (this figure can be compared with Figure 6-14 of SKB (2010a)). It is particularly notable that the releases cia the Q3 pathway are signficantly lower than calculated by SKB (noting the need to adjust the latter for the use of a distributed rather than basic LDF).

On the basis of these calculations, AMBER was considered to represent this SKB results for the far-field quite well, both in magnitude and trends in the calcuated releases. However, the trend discussed in Section 5.1.2, in which there appears to be less retention of contaminants in the geosphere matrix than calculated by SKB, is again evident in the results leading to higher releases calculated by AMBER.

Figure 27: Far-field Releases via the Q1, Q2 and Q3 Pathways (Deterministic Case, Normalised to a Single Canister Failure)

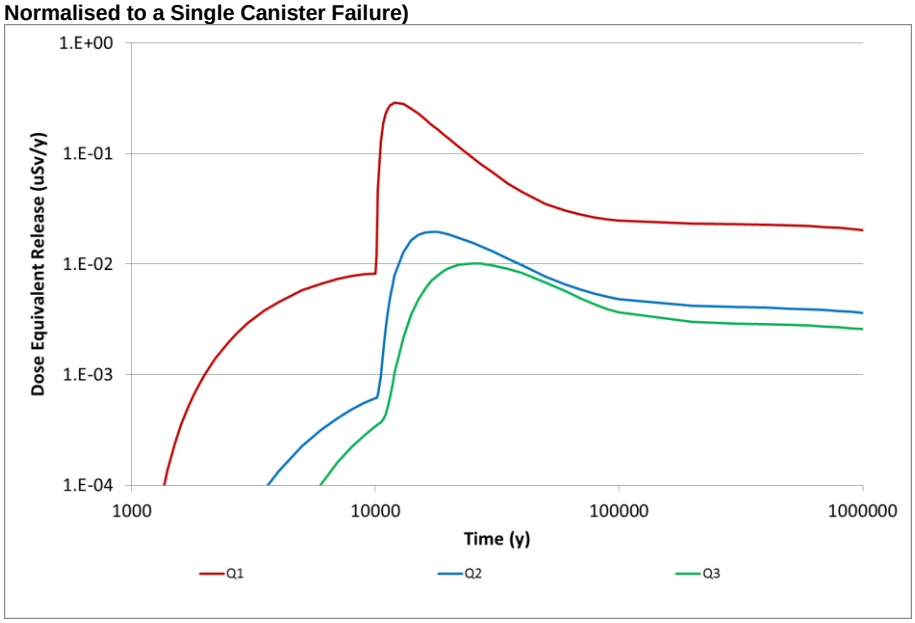

5.3. Case C

5.3.1. Near-Field

Case C considers an initial, large opening in the copper shell and in the cast iron insert for all canisters. The buffer remains intact, and the case is intended to explore the significance of the presence of the canister in controlling radionuclide transport. In relation to reference assumptions about the system performance, it is highly conservative in two respects – firstly, it assumes that, by some mechanism, the canister fails almost immediately after emplacement, and secondly, the case assumes that all canisters are affected. The case is thus more extreme than Case B, in that contaminant transport can occur straight away.

The model implementation in AMBER was achieved primarily by setting the delay time and time until a "large" defect occurs to the notional value of 100 y. The calculated dose equivalent releases from the near-field are presented in Figure 28 and Figure 29. The former compares SKB's results, from a probabilistic evaluation, with the results calculated with the deterministic AMBER model, which used median properties for sampled parameters. Figure 29 shows the results that were gained when a probabilistic calculation was undertaken with AMBER, although it should be noted that the AMBER calculation was for to a subset of the realisations, selected on the basis that they resulted in releases to the surface (see discussion in Section 3.2.2).

The general form of both deterministic and probabilistic AMBER results closely resembles those presented by SKB (2010a) in Table 6-63. The probabilistic results, in particular, agreed well with SKB's results for most radionuclides. Notable differences can be seen for shorter lived radionuclides such as Sr-90 and Cs-137 (about a factor of four difference) as well as Ag-108m (AMBER results around a

factor of two greater than SKB). The dominant factor influencing the releases from the near-field was the equivalent flow rate, as can be seen in Figure 30. By comparison, other parameters, including factors such as the Fuel Conversion Rate and solubility of elements, were less influential.

Figure 28: Comparison of Dose Equivalent Releases from the Near-Field for Case C, Calculated by AMBER (Deterministic Calculation) and SKB (Probabilistic)

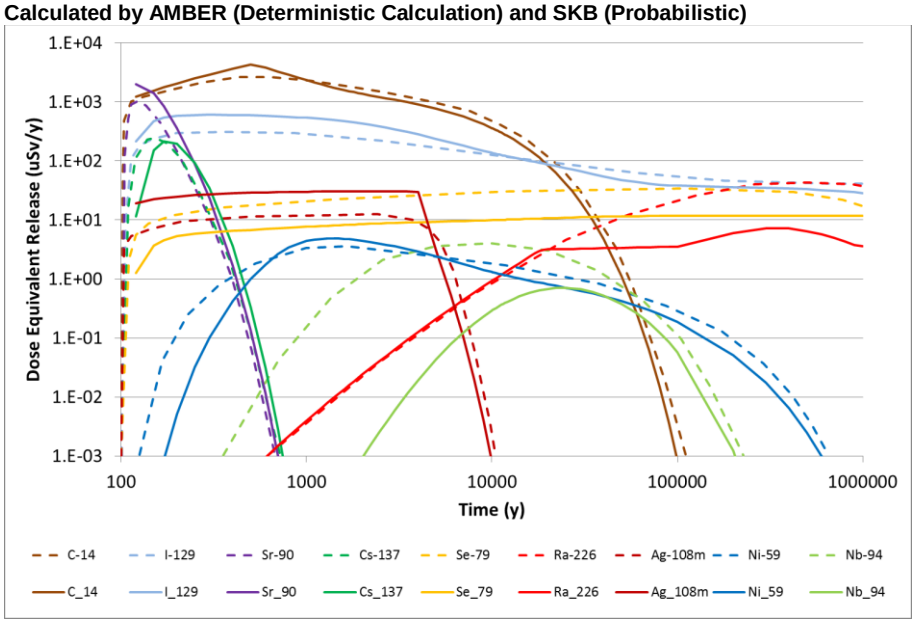

Note: * Dashed lines are SKB results, solid lines are AMBER results.

Figure 29: Comparison of Dose Equivalent Releases from the Near-Field for Case C, Calculated by AMBER (Probabilistic) and SKB (Probabilistic)

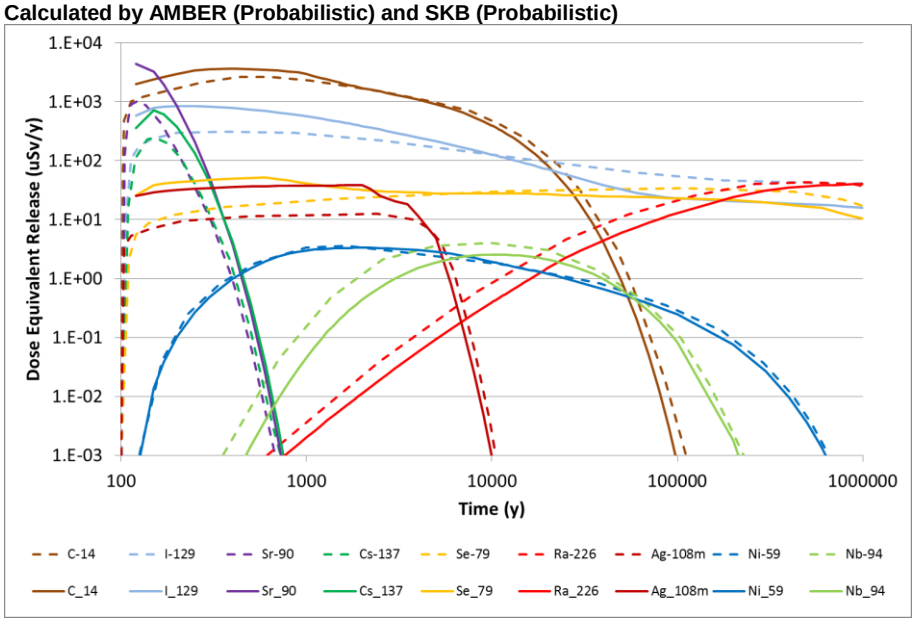

Note: * Dashed lines are SKB results, solid lines are AMBER results.

The good agreement with SKB results for the near-field releases from Case C indicate that the conclusions drawn by SKB for this case are sound. The AMBER analysis indicates that when the canister is not present the dominant factor controlling the near-field releases was the equivalent flow rate into the Q1 fracture.

Figure 30: Influence of Equivalent Flow Rate on the Dose Equivalent Releases from the Near-Field for Case C

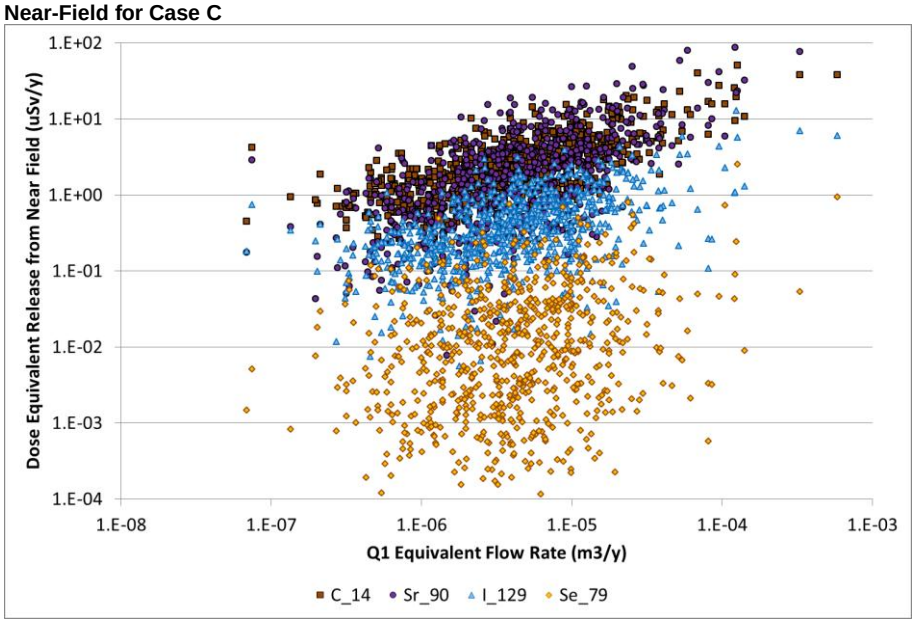

5.3.2. Far-Field

It can be seen from Figure 31 that there was a similar degree of agreement in the AMBER and SKB results for the far-field releases. For most radionuclides the agreement is reasonable at times greater than about 10,000 y, but at earlier times AMBER calculated a significantly greater release from the far-field than SKB's results shown in Figure 6-64 of SKB (2010a). This is similar to the trend observed in Case A and B, for example, and discussed in Section 5.1.2.

Figure 31: Comparison of Dose Equivalent Releases from the Far-Field for Case C, Calculated by AMBER and SKB (Probabilistic Calculations)

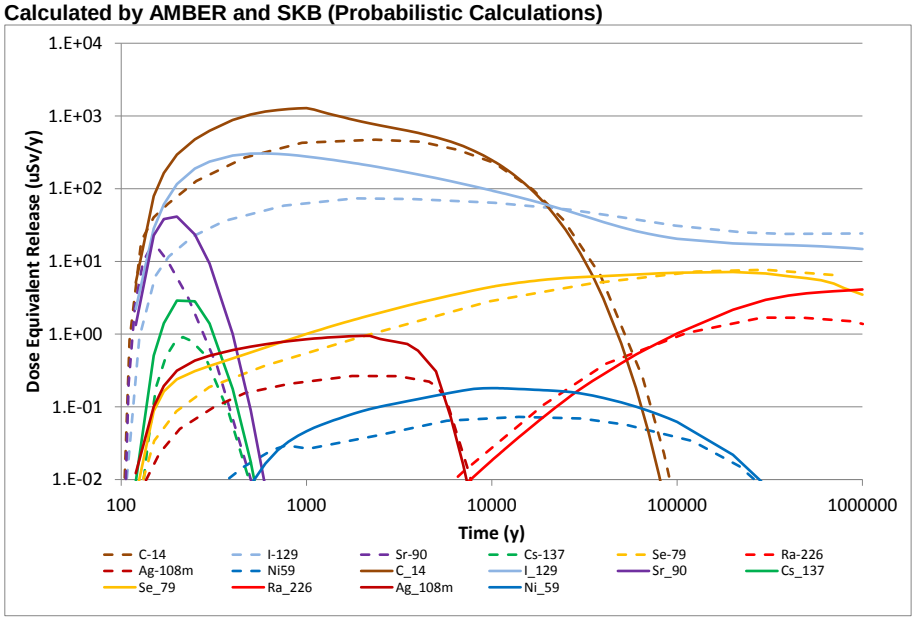

Note: * Dashed lines are SKB results, solid lines are AMBER results.

Of the results shown in Figure 31 it can be noted that there was good agreement for radionuclides like Se-79 and Ra-226 which are solubility limited, but less good agreement for Ag-108m (although still within a factor of about five). Differences were also noted with short-lived radionuclides such as Sr-90 and Cs-137 which appear to be related to a greater flux of the contaminants in the first few hundred years.

It can be concluded that the results, which agree reasonably well with SKB's calculations, indicate that the geosphere is less significant than the near-field in determining the results for Case C. Nevertheless, as with other cases, the AMBER model appears to lead to greater releases from the far field. This is most likely to be related to less retention of contaminants in the geosphere matrix.

5.4. Case D

5.4.1. Near-Field

Like Case C, this case postulates the presence of a large hole in all canisters occurring after 100 y, but here the adjacent buffer is assumed to be missing in all deposition holes (buffer above and beneath the hole is, however, assumed to remain present). The missing buffer was represented in the same way in AMBER as in Case A. Consistent with SKB (Section 6.5 of SKB (2010a)), solubility limitation was only applied to uranium and thorium isotopes, and contaminant release via the Q2 and Q3 pathways was not represented. The result is that the release from the near-field is controlled by the rate of contaminant release from the fuel and the flow rate through the deposition hole. In this case the buffer is absent at the fracture interface so no account has been taken of fracture resistance. Transport into the fracture was thus assumed to be determined by the equivalent flow rate alone.

The calculated dose equivalent release from the near-field is presented in Figure 32 and Figure 33. These compare AMBER results calculated with a deterministic and probabilistic model (respectively) with SKB's results.

The deterministic and probabilistic calculations can be seen to give similar results. In both cases, the agreement with SKB results was very good for all radionuclides and all times. Further analysis of the results showed that, for all radionuclides, a key process controlling radionuclide release was the equivalent flow rate (see Figure 34). Fuel conversion rate was also influential for those radionuclides for which there was no significant instantaneous or corrosion release fraction. This is obvious for Pu-239 and Ra-226, which can be seen to have a much lower dependency on the equivalent flow rate, but a much stronger dependency on the Fuel Conversion Rate, shown in Figure 35.

The case is similar to Case A, but in the agreement between the results is significantly better. This suggests that the AMBER model of the early phases of the system evolution is very similar to the SKB model, but that there may be differences in slower processes that become evident on longer timescales. Because all calculations for Case D assume a rapid and early release of contaminants from the canister, with no sorption and solubility only applying to U and Th, there are few other factors influencing the subsequent releases from the near-field. Furthermore, in this case (unlike Case A) all realisations share the same timing for the breach of the

canister. This means that the influence of other sampled parameters can much more readily be explored, as illustrated by the scatter plots.

Figure 32: Comparison of Dose Equivalent Releases from the Near-Field for Case D, Calculated by AMBER (Deterministic Calculation) and SKB (Probabilistic)

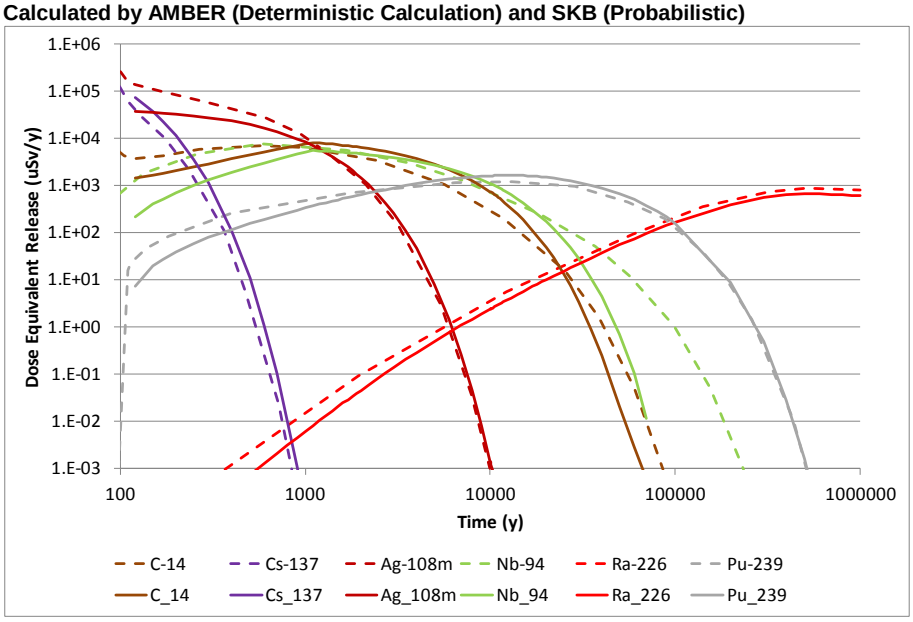

Note: * Dashed lines are SKB results, solid lines are AMBER results.

Figure 33: Comparison of Dose Equivalent Releases from the Near-Field for Case D, Calculated by AMBER and SKB (Both Probabilistic)

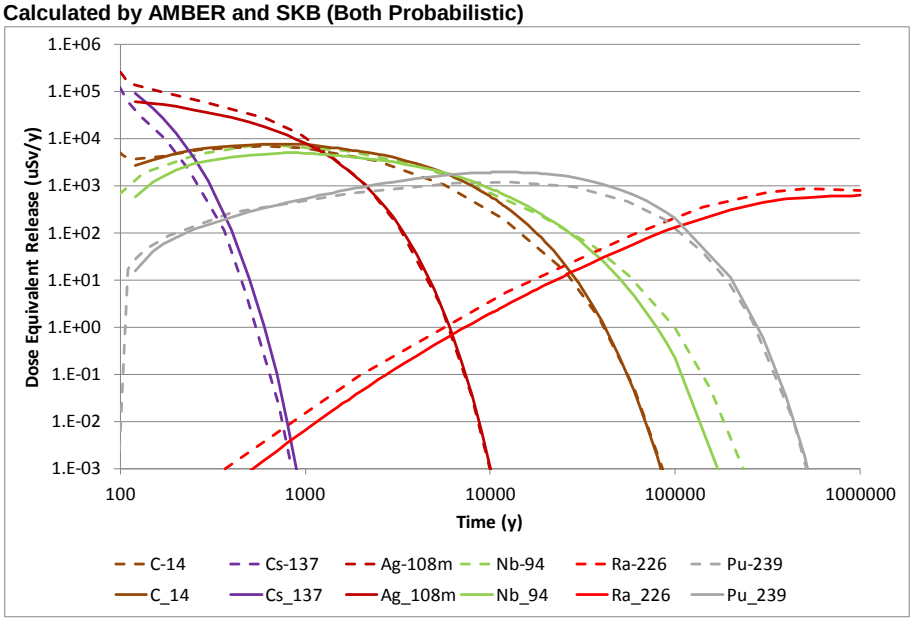

Note: * Dashed lines are SKB results, solid lines are AMBER results.

Figure 34: Influence of Equivalent Flow Rate on the Dose Equivalent Releases from the Near-Field for Case D

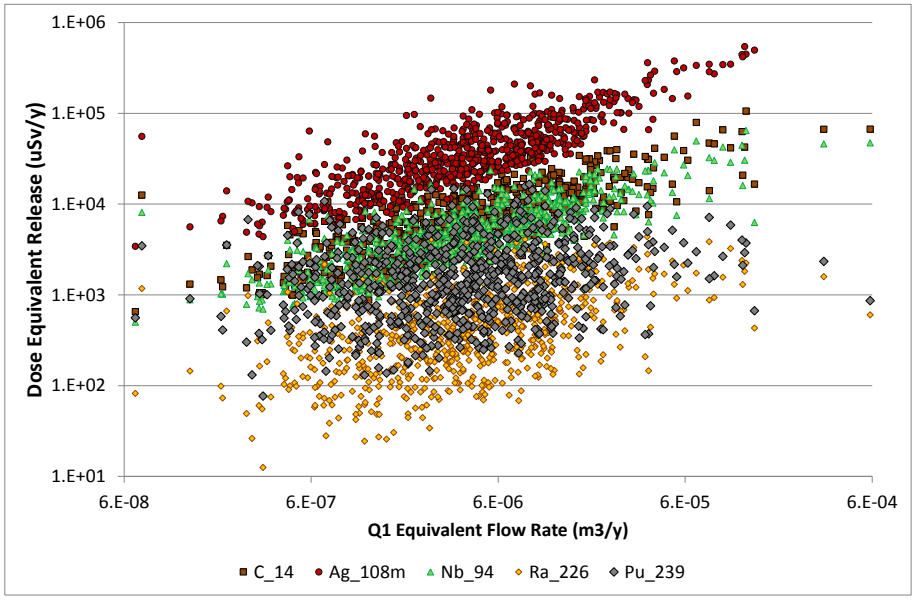

Figure 35: Influence of Fuel Conversion Rate on the Dose Equivalent Releases from the Near-Field for Case D*

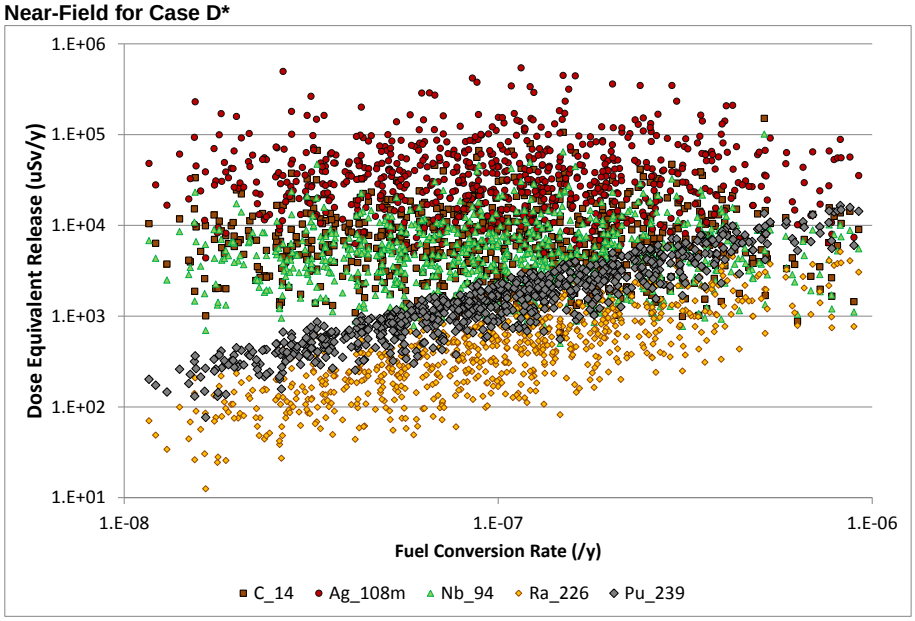

5.4.2. Far-Field

The dose equivalent releases from the far-field calculated with the AMBER deterministic and probabilistic model are presented in Figure 36 and Figure 37, where they are compared with the SKB results given in Figure 6-66 of SKB (2010a).

For this case the results of the deterministic case showed limited agreement with the SKB results. For all radionuclides, there were relatively small releases in the first few thousand years, compared with SKB's results (which even show a release of Cs-

137 from the far-field after a few hundred years). There was a degree of agreement on longer timescales. Results for unsorbed radionuclides (C-14 and I-129) were similar after about 10,000 y, and, after 100,000 y Se-79 (which exhibits a small degree of sorption) also approached the SKB results. However, for the sorbed radionuclides the peak concentrations were much lower than calculated by SKB. This is considered to be because the median values for key geosphere properties (used in the deterministic case) are significantly lower than the mean of the distributions used the probabilistic case. This can be expected, as the parameter distributions typically cover a wide range of values and are log-based. As a result, an arithmetic mean will tend towards a significantly greater value than the median of the distribution, and indicate higher releases for parameters sensitive such parameters.

Figure 36: Comparison of Dose Equivalent Releases from the Far-Field Calculated by AMBER (deterministic case) and SKB – Case D

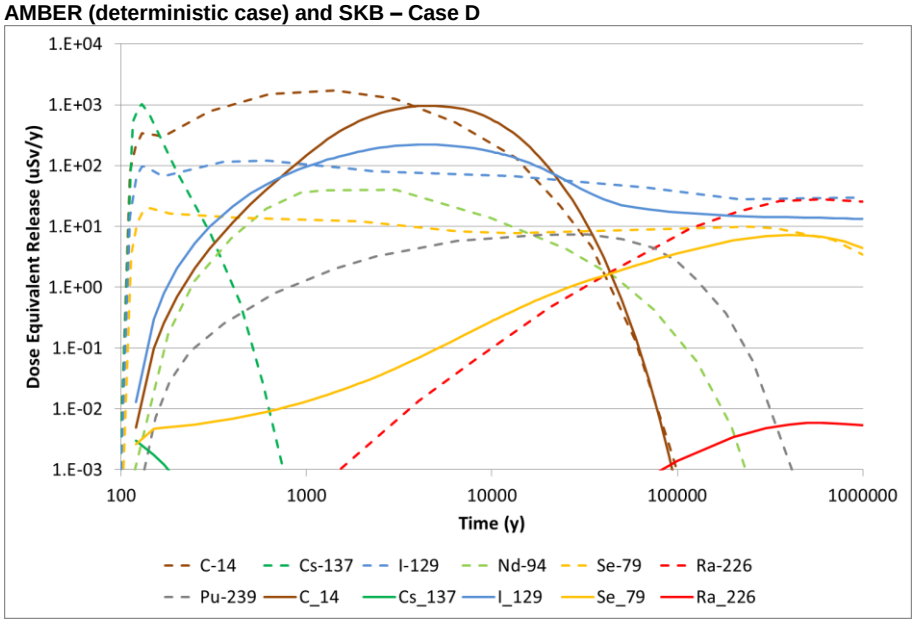

Note: * Dashed lines are SKB results, solid lines are AMBER results.

By contrast, the mean of the results calculated with the probabilistic implementation of the model in AMBER agreed well with SKB's results (see Figure 37). The calculated releases of C-14 and Ra-226 from the far-field were very similar, with less than a factor of two difference. Releases of other radionuclides also showed good agreement and were within a factor of 3 – 4. This supports the hypothesis that the difference in results lies in differences between median and mean values for parameter distributions concerned with far-field transport.

An investigation of model sensitivity showed that the combination of the substantial number of wide parameter distributions can lead to very large ranges in calculated far-field releases, with no one parameter dominantly controlling the fluxes. (Whilst it should be noted that the AMBER calculations did not apply correlations between any sampled parameters, there is no reason for key parameters such as sorption coefficient, matrix diffusion coefficient and advective travel time to be strongly correlated.) Figure 38 shows that even a strongly sorbed radionuclide like Pu-239 was not obviously correlated with sorption coefficient, but that the calculated far-field releases vary over a large number of orders of magnitude. Figure 39 compares the geosphere travel time with the calculated far-field release and shows that although there is some degree of dependency on this parameter for unsorbed or low

sorption radionuclides (C-14, I-129 and Se-79), it was not strong and there remains a substantial spread in values due to the influence of other parameters. No significant dependency of the dose equivalent release on effective diffusion coefficient for rock was found when this parameter was examined.

Figure 37: Comparison of Dose Equivalent Releases from the Far-Field Calculated by AMBER (probabilistic case) and SKB – Case D

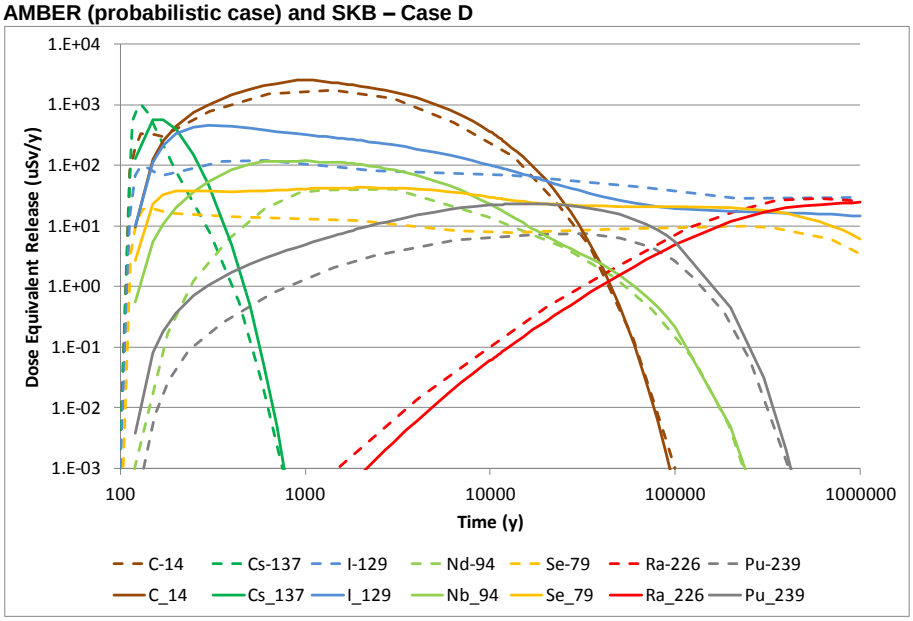

Note: * Dashed lines are SKB results, solid lines are AMBER results.

Figure 38: Influence of Sorption Coefficient for Radium in Rock on the Dose Equivalent Release from the Far-Field for Case D

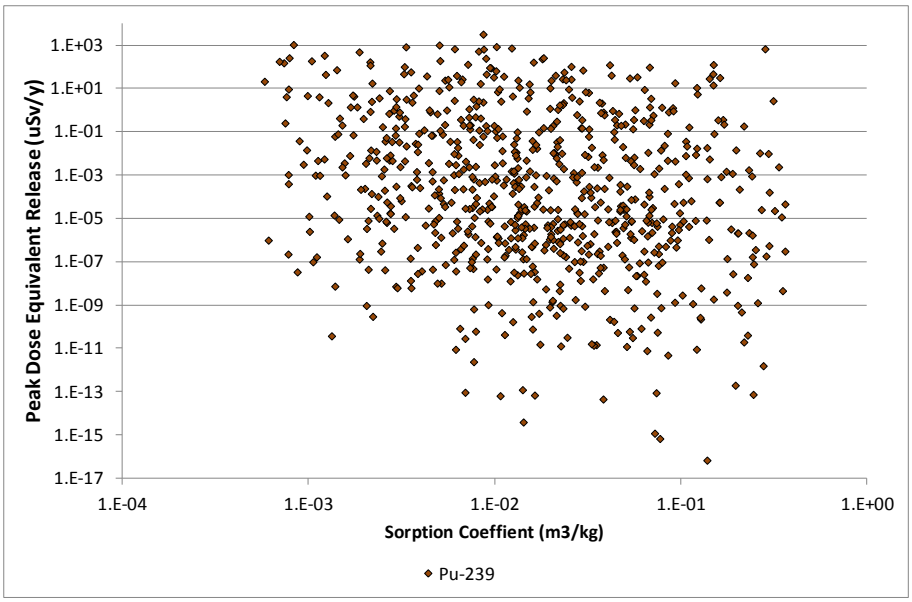

Figure 39: Influence of Geosphere Travel Time on the Dose Equivalent Release from the Far-Field for Case D

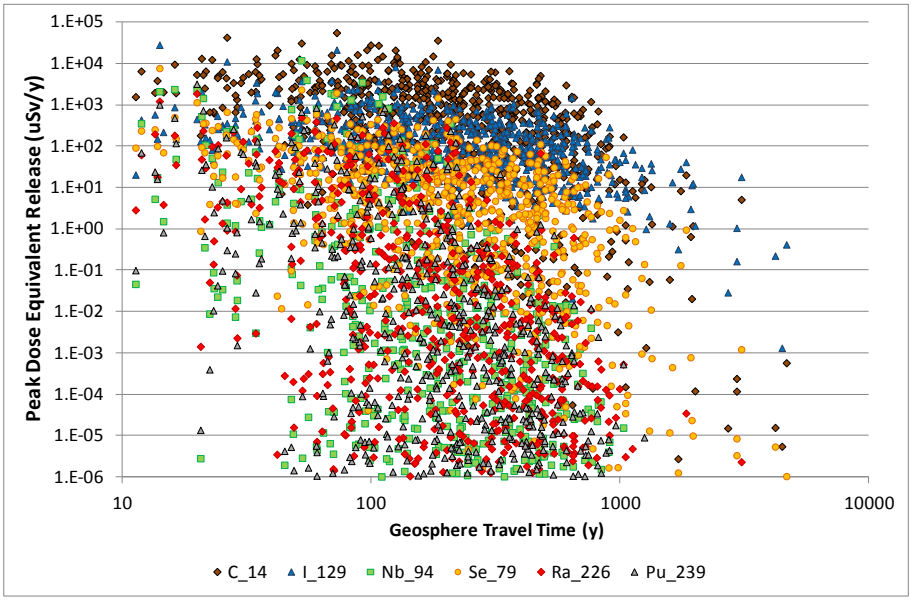

Note: No dose equivalent releases of less than 10^{-6} µSv/y have been plotted, in order to enable a reasonable scale to be applied for the y-axis

5.5. Case E

5.5.1. Near-Field

This case is a variation of Case C in which all canisters are assumed to have a large opening that occurs after only 100 y, but the buffer remains intact. The additional feature of this case is that all radionuclides are assumed to be released rapidly from the fuel and cladding, such that after 100 y all radionuclides have been released into water filling the canister void. The key difference is that in this case there is no control of radionuclide releases due to corrosion or fuel conversion. This means that, particularly at times of more than a few thousand years, the primary controls on releases are related groundwater flow, solubility and sorption rather than the release of contaminants from the fuel matrix. Clearly, this is a very extreme case as it removes all of the barriers and leads to very large dose equivalent releases.

The significance of solubility constraints on individual radionuclides has been illustrated by the calculated "availability" of contaminants for release from the canister void (i.e. the fraction of the total inventory that is below the solubility limit and thus "available" for release in groundwater). The results calculated by the deterministic AMBER case have been shown in Figure 40. Solubility limitation was a controlling factor in the releases of key radionuclides such as Se-79 and Ra-226. For example, the availability calculated by AMBER of Se-79 for release from the canister was much lower in Case E ($5\ 10^{-5}$) compared with 0.01 in Case C, in which the concentrations in the canister were controlled by the fuel conversion rate as well as solubility constraints.

The result is that the release of radionuclides associated with the fuel, in particular, was significantly different than that for Case C. This was most obvious for Ra-226

which, in other cases, gradually increased over time as a result of the gradual release of it and its long-lived parents, influenced by the fuel conversion rate. In this case, the release was almost constant over time, being dominantly controlled by solubility. Good agreement with SKB results was found for most radionuclides with both the deterministic implementation of the models in AMBER (Figure 41) and the probabilistic model (Figure 42). The deterministic model results can be seen to match SKB results (from Figure 6-67 of SKB (2010a)) very well for Sr-90, C-14 and Cs-137. For I-129, the results agreed well up to around 10,000 y. After this, AMBER calculated a declining rate of release as the inventory of the radionuclide in the near-field, in particular via the pathway to the Q1 fracture (see Figure 43).

Figure 40: Effects of Solubility Limitation on the Availability of Contaminants for Release from the Canister Void in Case E

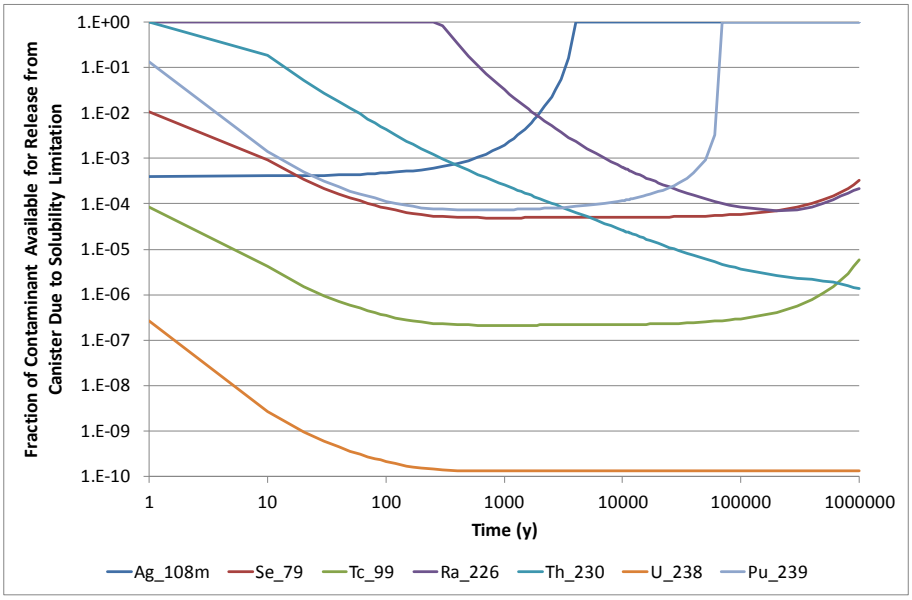

Figure 41: Comparison of Dose Equivalent Releases from the Near-Field for Case E, Calculated by AMBER (Deterministic Calculation) and SKB (Probabilistic)

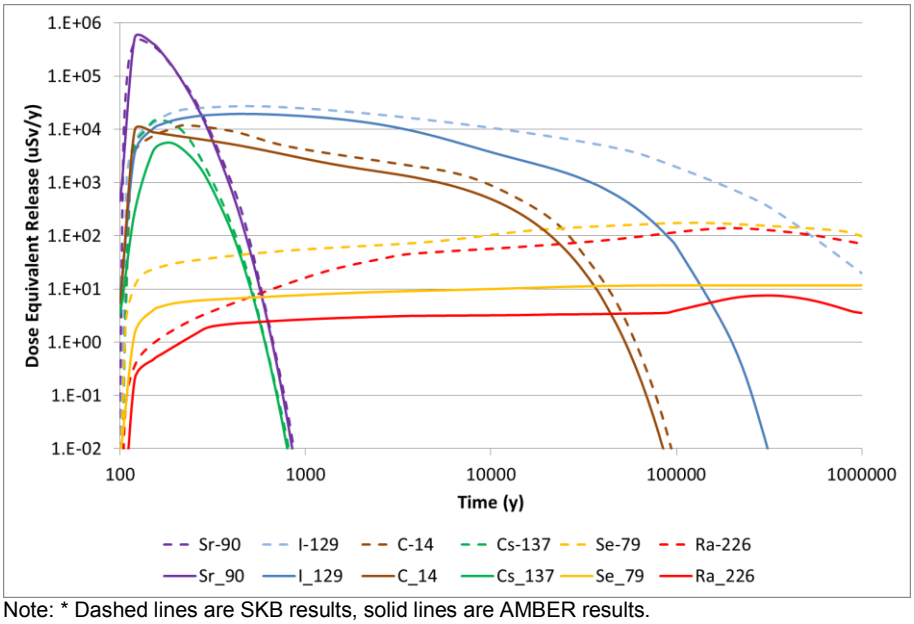

Note: * Dashed lines are SKB results, solid lines are AMBER results.

Figure 42: Comparison of Dose Equivalent Releases from the Near-Field for Case E, Calculated by AMBER and SKB (Both Probabilistic)

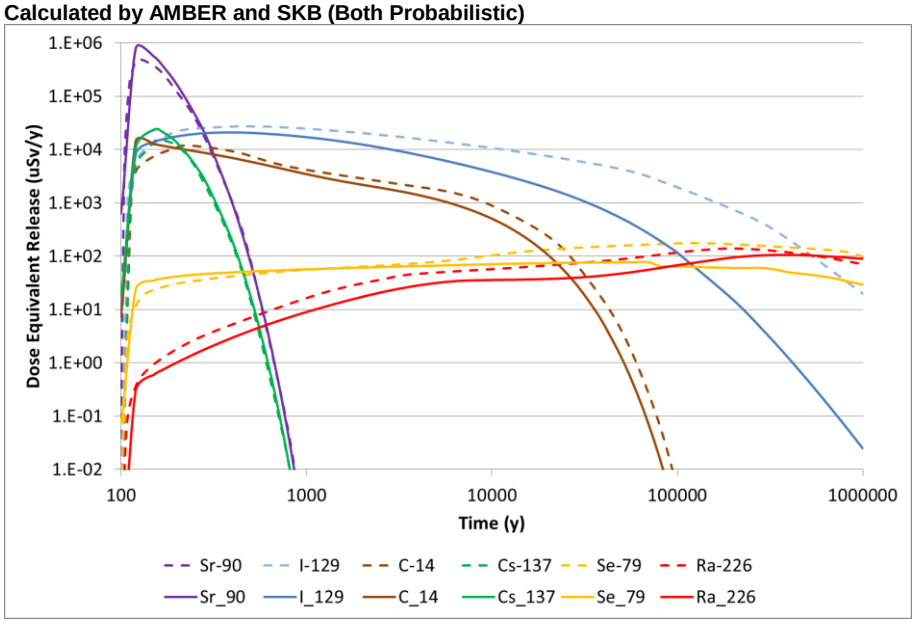

Note: * Dashed lines are SKB results, solid lines are AMBER results.

The other main difference observed with the deterministic calculation is in relation to Se-79 and Ra-226. As seen in Figure 40, the release of these radionuclides was controlled by solubility. The deterministic AMBER case used a median value for the solubility of elements, which in the case of Se-79 was 6.7 10^{-6} mol m^{-3}. This differed significantly from the mean value of the probability distribution of solubility for Se, which was 3.1 10^{-5} mol m^{-3}. The higher solubility value implies a greater rate of release of Se-79 would be seen in the mean of the probabilistic calculations. There are similar differences in the median and mean for Ra-226 solubility limits.

The results of the AMBER probabilistic calculation for Case E bear this out and demonstrated very good agreement with SKB results for all radionuclides except I-129, which again showed a more rapid decline than calculated by SKB. The distribution of the radionuclide in the deterministic version of the model (Figure 43) suggested that the difference lies in greater retention of the contaminant in the near-field and the rock matrix on a timeframe of 1,000 – 100,000 y.

The simplicity of the modelling of this aspect is such that it is unclear why such a difference was present. The radionuclide was assumed to be entirely released from fuel, and, as it is relatively mobile. I-129 would not therefore be expected to be retained in the near-field for long timescales. Nevertheless, the overall level of agreement between AMBER and SKB results for other radionuclides was good. The results for radionuclides other than I-129 were within a factor of 3, and the form of release is similar. For I-129, the discrepancy relates to the long-term, well after the peak release from the near-field has occurred.

The calculation results for the near-field releases confirmed that the dominant aspect controlling the flux of radionuclides for this case is the equivalent flow rate into the Q1 fracture. This is illustrated in the scatter plot shown in Figure 44, which is based on the results of the probabilistic calculations using the AMBER model.

Figure 43: Total Amount of I-129 in Parts of the AMBER Model as a Function of Time, for the Case E Deterministic Calculation (Single Canister Release)

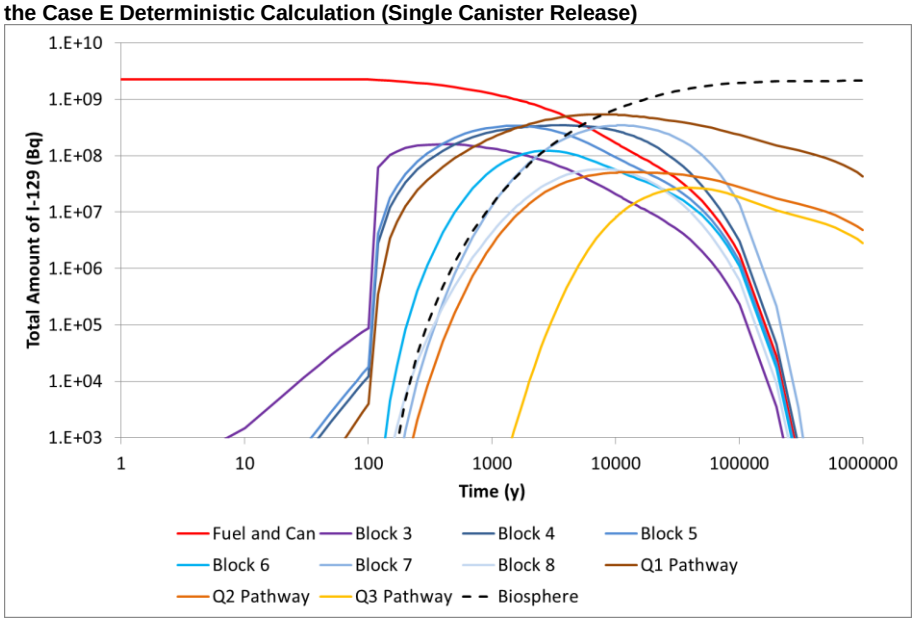

Figure 44: Illustration of the Influence of Equivalent Flow Rate for the Q1 Pathway on the Peak Dose Equivalent Near-field Release Calculated in the Probabilistic AMBER Model for Case E

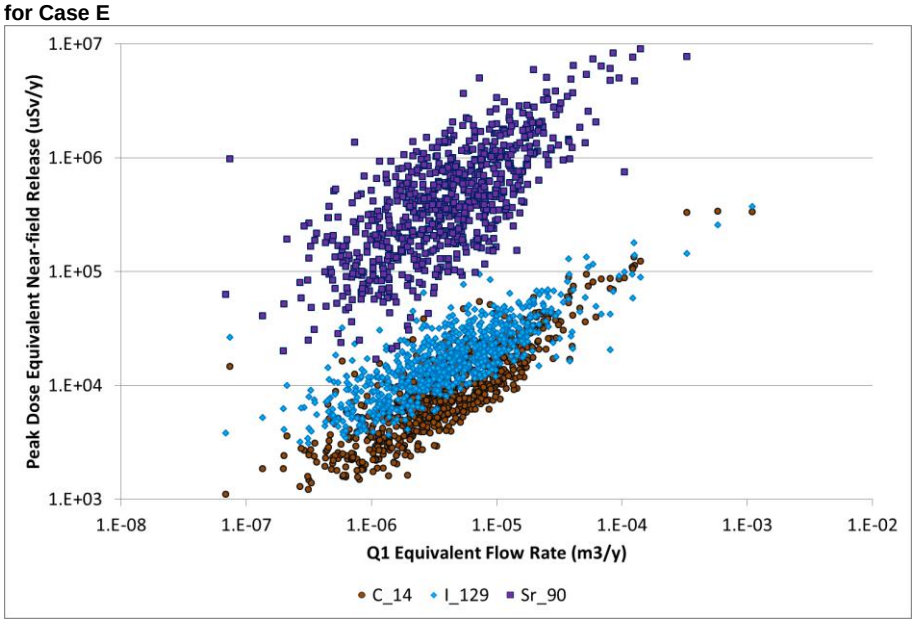

5.5.2. Far-Field

The dose equivalent releases from the far-field calculated by AMBER were expected to match well with those presented by SKB (see Figure 6-68 (SKB, 2010a)) given the similarities in the results for the near-field release. However, at earlier times and for sorbed radionuclides there was less agreement, which was particularly noticeable with the AMBER deterministic case. As has been noted in respect of other calculation cases, this is likely to be related to the differences in the

mean value of geosphere parameter distributions and the median used in the deterministic case.

The results obtained from the probabilistic calculations with the AMBER model were, however, much closer to those calculated by SKB and shown in Figure 6-69. The results for C-14, C-137 and Ra-226 match very well, and I-129 agrees well for the first 1,000 y before the AMBER model calculates lower releases than SKB. For Se-79, AMBER indicates a significant tendency for a rapid release in the first 1,000 y, compared with the SKB calculations. The main factor that could result in such a condition is the solubility limit for the element. The other notable difference is that the release of Cs-137 calculated by AMBER is nearly an order of magnitude larger after about 200 y, before declining in the same way as SKB's results.

Figure 45: Comparison of Dose Equivalent Releases from the Far-Field for Case E, Calculated by AMBER and SKB (Both Probabilistic)

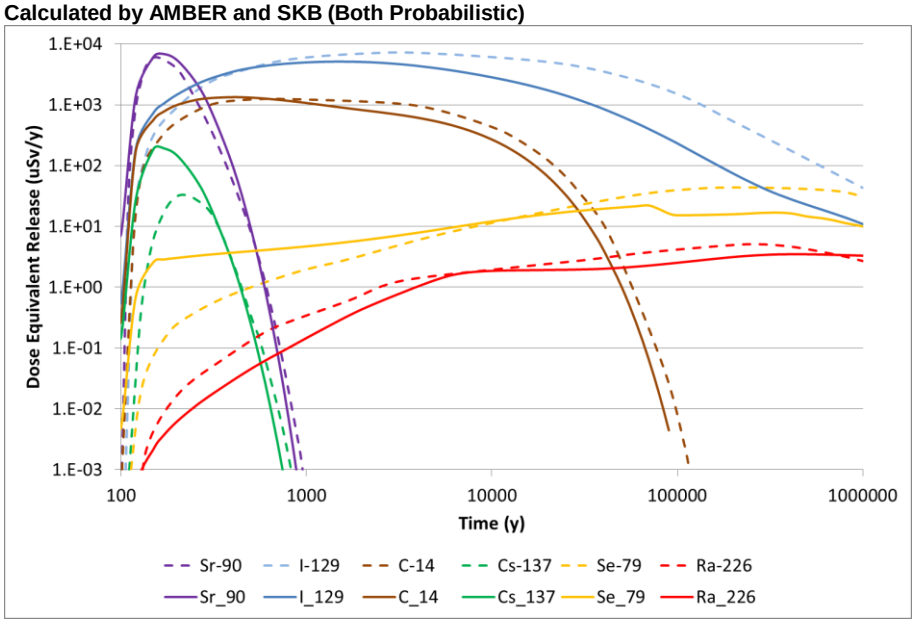

Note: * Dashed lines are SKB results, solid lines are AMBER results.

As with other calculation cases, there are some notable differences that can be observed for particular radionuclides, but the overall form and magnitude of the releases calculated by AMBER agree well with SKB's results. As with other calculation cases, the releases from the geosphere are largely dictated by aspects of the near-field. The dominant aspect influencing the calculated release from the far-field is the equivalent flow rate into the Q1 pathway. This is demonstrated in the scatter plot shown in Figure 46.

Figure 46: Illustration of the Influence of Equivalent Flow Rate for the Q1 Pathway on the Peak Dose Equivalent Far-field Release Calculated in the Probabilistic AMBER Model for Case E

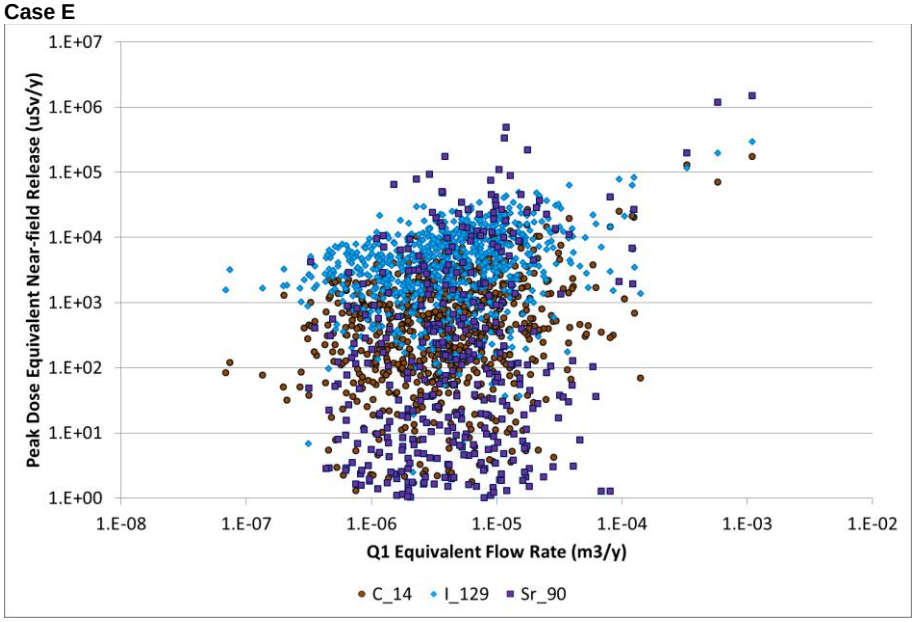

6. Discussion of Key Findings

6.1. Implementation of the Independent Assessment Model

The development and implementation of the SKB model in AMBER required a considerable period of prototyping and model development. This was due to some lack of clarity in, and structure to, the presentation of SKB's models and data in the relevant reports (SKB 2010a; 2010b; 2010d). Key points are summarised in this section.

6.1.1. Models

The design of the radionuclide transport model was mainly gained from SKB's description contained in Appendix G of SKB (2010a). This proved to be a largely sufficient specification for the independent implementation of the near-field model in the AMBER code. The model structure was described in adequate detail, although there were some areas in which a degree of interpretation was needed. For example:

- The application of solubility limits was unclear (by what method, and in what parts of the model);
- It was necessary to decide whether to apply constant a fractional release rate or a adopt a congruent release representation of fuel conversion and corrosion (SKB's documentation implies a fractional rate for fuel conversion and congruent release for corrosion);
- The representation of diffusion transfers within media required some interpretation, in particular at interfaces between free water and porous media, as well as the assumptions made by SKB in respect of selecting diffusion length;
- The basis and application of concepts such as fracture resistance, equivalent flow rate, and the representation of spalling could have been more clearly described.

Whilst these aspects were believed to be resolved in the AMBER model implementation, through a process of progressively developing and refining the model, there remain some differences in the calculated releases from the AMBER model which have not been fully explained. It is believed that these relate to diffusion through the buffer to Q2 and Q3 pathways, because the model is sensitive to the representation of the process. The very limited set of results available in SKB (2010a) does not enable investigation of contaminant transport through this part of the disposal system model.

A corresponding description of the modelling approach for the far-field was not available, although some details of the FARF31 were presented in SKB (2010d). Conceptually, the model for this part of the system is simple. In the AMBER model, each pathway (Q1, Q2 and Q3) was represented as a 1-dimensional advective pathway with associated matrix diffusion compartments. Nevertheless, whilst this is mathematically simple to implement, suitable choices need to be made in its representation in a compartment model, in particular with regard to discretisation and the appropriate specification of compartment dimensions. This aspect was

investigated (see Section 4) and it was shown that the representation of matrix diffusion, in particular, was an aspect to which the model results can be sensitive. The discretisation of the AMBER model's matrix diffusion zone into six compartments of increasing thickness was made on the basis of existing experience. The limited information on the role of the rock matrix in the SKB results did not enable the validity of this implementation to be fully tested, other than by interpretation of the far-field dose equivalent releases.

6.1.2. Data

The primary source of data was the SKB Data report (SKB, 2010b), which is a detailed document. The analysis and justification of data presented in that report is clearly necessary as part of the safety case as a whole, but as a compilation of information for modelling purposes the format adopted by SKB (2010b) left some areas open to interpretation. For this reason, a supporting document (SKB, 2011), which compiled the specific data choices used for the key calculations in just a few pages, was a valuable point of reference. With these documents, all key deterministic data were identified. The source of information used in the AMBER model has been recorded in Appendix B for reference. It is noted, however, that until the compilation of data was obtained, the identification of the specific values used in SKB's calculations was time consuming.

It was necessary for AMBER to use the results of detailed modelling (e.g. ConnectFlow output) in the same way as SKB's radionuclide transport codes in order to calculate probabilistic results. The use of SKB's supporting model output (e.g. solubility values, hydrogeological modelling output) with the AMBER model proved to be successful. However, some of these data were clearly important to the model results (e.g. equivalent flow rates, or corrosion failure times) but had to be treated as "black box" model results. A better understanding of the basis of these values (which in many cases are key factors in controlling the model's calculated releases) would be of benefit in understanding some of the more detailed aspects of the model behaviour.

It is also noted that considerable emphasis was placed in SKB's calculations on very large numbers of realisations to represent the spatial variability of the repository environment. As such a large number of calculations were not practical in the available time, reduced datasets were assessed in the AMBER probabilistic calculations. Whilst there were some differences between the results with the reduced number of realisations and the complete data set, these were of relatively limited significance. Indeed, in most regards deterministic calculations provided an adequate representation of the system's behaviour and greater emphasis on deterministic calculations would have been of benefit. Deterministic cases are generally easier than probabilistic analyses to present, interpret and explore.

6.2. Results Obtained

6.2.1. Implications of the Results for the Safety Case

As has been noted, the independent calculations required a relatively significant phase of prototyping in order to refine certain aspects of the model implementation.

This process was useful in gaining an understanding of the model performance and behaviour. Areas of notable sensitivity were found to be:

- the representation of radionuclide releases at key points in the model (the canister to the buffer, and buffer to fracture);
- diffusion in the near-field towards Q2 and Q3 pathways; and
- matrix diffusion in the geosphere.

These aspects were highlighted in prototyping work, which found that for sufficient agreement with the SKB results it was necessary to represent fully the Q2 and Q3 pathways and the matrix diffusion component of geosphere transport. With these model components implemented in the AMBER model the calculations agreed with SKB's in indicating that the key factors controlling the performance of the model were:

- the integrity of the canister;
- the fuel conversion rate and elemental solubility, which control the release from a damaged canister;
- the flow rate into the fracture; and
- matrix diffusion in the geosphere.

An important feature of this conclusion is that – with the exception of the canister itself – the key controls on radionuclide migration were features that are intrinsic to the geological environment (fracture properties and geochemistry). The key part of the repository's engineered system to which a degree of reliability and confidence needs to be assigned is clearly the canister itself, although the results indicated that canister failure on timescales of tens of thousands of years (e.g. Case A) would not lead to releases that approach safety criteria. Furthermore, it was noted that in all calculations a deliberately cautious approach has been adopted when defining key parameter values, even in the assignment of probability distribution functions. In respect of the calculations assessed in this study, the assumptions adopted for aspects of the barrier function were deliberately extremely cautious (to the point of being implausible) and as such the results were treated purely as performance indicators that aid system understanding.

An appropriate representation of the processes that dominantly control radionuclide release led to results that agreed well with SKB's results for most radionuclides and calculation cases. In some specific cases the difference was greater, but the dominant radionuclides and peak releases generally agreed to within a factor of five, and often considerably better. This was largely a reflection of the characteristics of the key radionuclides. The behaviour of I-129, Se-79 and Ra-226 in particular was determined by either the Fuel Conversion Rate and/or solubility limitation. C-14 was also a dominant radionuclide, being released from the fuel rapidly (with both a significant instant release fraction and a significant corrosion release fraction), and being mobile in the engineered and geological environments.

By comparison with the near-field, the calculations suggest that geosphere offers relatively little in terms of a barrier to radionuclide transport for most radionuclides in most calculation cases. This is because the travel time by advection is very short in relation to the timescales of radionuclide releases and their half-life, and the flux of contaminants was typically dictated by controls in the near-field. Nevertheless, it was found that matrix diffusion had a notable influence the releases of some radionuclides from the geosphere, including Se-79 and Ra-226. In order to gain good agreement with SKB's results for radionuclides that exhibit sorption an appropriate representation of the rock matrix was considered to be important. Limited information on the distribution of radionuclides in the geosphere meant that

it was not possible to explore this aspect in detail, but it was considered likely to be responsible for some unresolved differences between the AMBER and SKB results.

6.2.2. Interpretation of Barrier Functions

The main objective of the suite of five calculation cases was to inform on the role of barriers in providing safety. In this respect, the absolute values of calculated dose or release rate were only important as a point of reference between the cases, as none represents a plausible "scenario" (not least because all cases represent barrier failures for all deposition holes simultaneously).

The calculation cases selected by SKB, as a suite, provide comprehensive coverage of the main barriers in the disposal system. No obvious alternative calculation cases could be identified, because the calculation cases defined by SKB adopted extreme assumptions for each component of the barrier separately and in combination. Additional calculation cases that examine partial or gradual failure of barriers are, in the context a "what if" analysis, uninformative. For this reason, no additional calculation cases were defined in this study; instead effort was applied to examining the suite of cases defined by SKB through additional calculated endpoints such as the amounts of radionuclides in different parts of the model, or scatter plots used to determine the importance of particular parameters.

Using this form of analysis, the independent calculations undertaken for the five cases support the outcome of SKB's analysis. The AMBER results, whilst not agreeing exactly with SKB's results, provide a sufficient degree of verification of the analysis to provide confidence in its conclusions. No significant discrepancies were identified, although a number of minor issues were identified and have been discussed in the following section.

The canister itself remains the primary and dominant engineered barrier to the safety performance of the system. This was demonstrated by Case A, in which there is no function provided by the buffer in resisting transport to the Q1 fracture after canister failure. On the timescales over which the canister can be relied to perform (of the order of several tens of thousands of years or greater) other processes are relatively rapid (e.g. corrosion, diffusion in the barrier, transport in the geosphere). In this respect, the factor controlling the overall magnitude of the radiological consequences is the number of canister failures.

An extreme illustration of the failure of all engineered barriers was provided by Case E, in which no retention of radionuclides within the wasteform occurs, and the only barrier to its release was the resistance offered by the fracture. This enabled a rapid release of C-14 and I-129 in particular, and – by comparison with the other results – illustrates the importance of the fuel conversion rate in controlling releases. The fuel itself is sometimes not considered to be barrier, but its properties, in terms of very gradual conversion, provide a key control on the near-field release rate for many radionuclides.

The results for Cases B, C and D highlighted the role of barriers in controlling releases in the first few thousand years. These cases were similar in magnitude at times greater than 10,000 y indicating that the barrier functions of the near-field tend to control the timing of releases more than the absolute magnitude on long timescales. As greater reliance can be placed on the function of the key barriers in the relatively short term, this finding indicates that a degree of redundancy in the

barrier on longer timescales will not substantially reduce the safety performance of the system.

It is notable that in all calculation cases key radionuclides included C-14, Se-79, I-129 and Ra-226. These radionuclides all have characteristics that contribute to the potential for release in the medium and long term. C-14 is important because it is relatively rapidly released into the canister void, and is thereafter assumed to be mobile in the buffer and geosphere. Se-79 is long lived and controlled by solubility limitation, but once released from the canister is relatively mobile and therefore can rapidly migrate to the geosphere. I-129 releases are controlled by fuel conversion, but it is otherwise highly mobile. Finally, Ra-226 is important because, whilst it is short-lived in the context of the overall assessment timescales, it is constantly generated by solubility limited parents in the near-field, and is eluted from the canister due to its higher solubility and lower sorption.

As has been noted previously, the geosphere did not appear to provide a significant barrier function for most key radionuclides. The exception was where sorption in the rock matrix was modelled as being significant. For radionuclides such as Se-79 and Ra-226, matrix diffusion appears to be an important factor, albeit less significant than the near-field barriers.

6.2.3. Key Discrepancies and Issues

Overall, the independent calculations show good agreement with SKB's results, but there are a number of aspects that have not been fully resolved. These issues remain mainly because of the limited range of results presented by SKB (2010a) which can be used to compare AMBER model output with. In particular, additional results that show the detailed behaviour of the system (e.g. calculated concentrations in the main parts of the system) would help in identifying the source of differences.

The key unresolved aspects of the system are as follows.

- In some the calculated releases of particular radionuclides showed less agreement than others. This is particularly notable in respect of near-field releases of Ra-226 in Cases A and B, and Ag-108m in Case C, for example. With the available data and results for comparison it was not possible to determine which specific characteristics of these radionuclides resulted in the differences.
- In most cases AMBER calculations of far-field releases were significantly greater than those calculated by SKB. Analysis of the AMBER results suggested that this was a result of less rapid diffusion into the rock matrix in the AMBER model, but this hypothesis could not be tested as the relevant model results were not published in SKB's documentation.

Nevertheless, it was found that most results from the AMBER calculations were within a factor of 2 – 5 of the SKB results, particularly at the point of peak release. Some differences were observed either at short- or long times, which are also anticipated to be related to the detailed representation of diffusion in various parts of the system. Overall, however, the good agreement with SKB results indicates that the AMBER model adequately represented the key processes.

7. Conclusions

As part of SSM's review of the "SR-Site" safety assessment an independent analysis has been made of a set of "what if?" calculation cases that explore the role of the near-field barriers in providing safety. SKB analysed five cases that illustrate the function of the canister and buffer by selectively removing them from the model. The results were not intended for comparison with safety criteria as the calculation cases represent implausible situations, but they do serve to demonstrate the influence of the engineered components on the behaviour of the system.

The analysis involved using SKB's documentation to recreate the radionuclide transport model independently in a separate contaminant transport code, AMBER. This proved to require a significant degree of prototyping and experimentation in order to establish whether any simplification of the models could be applied and still achieve adequate results, and also because some aspects of the model were not fully clear in the SKB reports. In particular, it was notable that much of the relevant information is distributed amongst several reports, which meant identifying the right model specification or data could take time. Nevertheless, the prototyping phase established that a complete implementation of the SKB radionuclide transport models was necessary, but that such an approach should yield results that agreed with SKB results to within a factor of 2 – 5 for most radionuclides.

The AMBER model was applied to each of the SKB cases in both deterministic and probabilistic mode. In deterministic mode, the AMBER model took SKB's recommended median parameter values. In probabilistic mode, the AMBER model sampled from the probability distribution functions defined by SKB as well as selecting values from pre-calculated sample files. The sample files were supplied by SKB, and are output from models that support the radionuclide transport calculations. These supporting models are concerned mainly with hydrogeological and geochemical aspects. SKB's probabilistic calculations used 6916 realisations, one for each deposition hole location. Because of computing time constraints, the AMBER model calculations were undertaken for a subset of around 1000 cases which led to radionuclide releases within the assessment timeframe (the remainder did not lead to a release and therefore effectively have no impact). Although there are obvious differences between the deterministic and probabilistic calculations, these are reasonably minor, and typically the deterministic case captured all the key features of the disposal system performance.

The evaluation of the comparative performance of the AMBER and SKB models was limited by the small selection of results presented by SKB for the cases under consideration. These were limited to presenting dose equivalent releases from the near-field and far-field. Nevertheless, for these performance measures, the AMBER implementation of all cases showed good agreement with SKB results for key radionuclides. These cases have common features in that they explore the importance of the canister on safety performance by examining the consequence of its absence on various timescales. Most results were within a factor of 2 – 5 at the point of peak release. Some differences were observed either at short- or long times, which are also anticipated to be related to the detailed representation of diffusion in various parts of the system. Overall, however, the good agreement with SKB results indicates that the AMBER model adequately represented the key processes.

The range of results provided a clear picture of the key aspects of barrier performance. The AMBER calculations agreed with SKB's in indicating that the key factors controlling the performance of the model were:

- the integrity of the canister;
- the fuel conversion rate and elemental solubility, which control the release of radionuclides from a damaged canister;
- the effective rate of release from the buffer into the fracture (the "equivalent flow rate"); and
- matrix diffusion in the geosphere.

The key part of the repository's engineered system to which a degree of reliability and confidence needs to be assigned is clearly the canister itself, although the results indicated that canister failure on timescales of tens of thousands of years (e.g. Case A) would not lead to releases that approach safety criteria. The main role of the buffer was to protect the canister by limiting the flow of groundwater and hence limiting the potential for corrosion. A further conclusion was that – with the exception of the canister– the key controls on radionuclide release from the near-field were intrinsic properties of the waste (fuel conversion rate) and the geological environment (fracture properties and geochemistry).

By comparison with the near-field, the calculations suggest that geosphere offers relatively little in terms of a barrier to radionuclide transport for most radionuclides. The exception was radionuclides that exhibit a degree of sorption, but are also potentially released in substantial amounts. For these radionuclides, matrix diffusion can have a notable influence. This aspect was a key area of difference between AMBER and SKB results. This may relate to the compartment sizes used in the matrix which may be larger than required for sorbed nuclides; the SKB results use a semi-analytic approach that does not require matrix discretisation. It was not possible to explore the issue in detail due to the limited range of results available. Nevertheless, this is a relatively minor aspect that is only relevant when the extremely conservative "what if?" assumptions are applied.

8. References

ANDRA. 2003. BIOSCOMP Project: Intercomparison Exercise between AQUABIOS, AMBER and MEPAS for the Calculation of the Transfers of Non-Radioactive Pollutants within the Biosphere. ANDRA Report Z RP 0ANT 03-029, December 2003.

Jones J, Vahlund F, Kautsky U and Kärnbränslehantering S. 2004. Tensit – a Novel Probabilistic Simulation Tool for Safety Assessments: Tests and Verifications Using Biosphere Models. SKB Technical Report TR-04-07, June 2004.

Little R H, Robinson P C, Humphreys P and Schneider J. 2003. The Application of the AMBER Software Tool to the Geological Disposal of Radioactive Waste. 6th Slovak-Czech Seminar on the Geological Disposal of Radioactive Waste, Piestany, 26-28 August 2003.

Little R, Dragolici F, Bond A, Matyasi L, Matyasi S, Naum M, Niculae O, Thorne M and Watson S. 2007. Preliminary Safety Analysis of the Baita Bihor Radioactive Waste Repository, Romania. Proceedings of the 11th International Conference on Environmental Remediation and Radioactive Waste Management ICEM2007, September 2-6, 2007, Oud Sint-Jan Hospital Conference Center, Bruges, Belgium.

Little R, Avis J, Garisto N, Humphreys P, King F, Metcalfe R, Penfold J, Ramlakan A, Suckling P, Towler G, Walke R, Walsh R, West A and Wilson J. 2011. Postclosure Safety Assessment. Quintessa Ltd. report for the Nuclear Waste Management Organization NWMO DGR-TR-2011-25 R000. Toronto, Canada.

Maul P R, Robinson P C, Broed R, and Avila R. 2004. Further AMBER and Ecolego Intercomparisons. SKI Report 2004:05/SSI Report 2004:01, Stockholm, January 2004.

Maul P R, Robinson P C, Avila R, Broed R, Pereira A and Xu S. 2003. AMBER and Ecolego Intercomparisons using Calculations from SR 97. SKI Report 2003:28/SSI Report 2003:11, Stockholm, August 2003.

Maul P R, Robinson P C, Bond A E and Benbow S J. 2008. Independent Calculations for the SR-Can Assessment: External Review Contribution in Support of SKI‟s and SSI‟s Review of SR-Can. SKI Report 2008:12.

Quintessa. 2013a. AMBER 5.7 Reference Guide. Quintessa report QE-AMBER-1 Versions 5.7. Quintessa Ltd, Henley-on-Thames, UK.

Quintessa. 2013b. Quintessa Limited Quality Manual. Version 3.4, August 2013. Quintessa Limited, Henley-on-Thames, United Kingdom.

Quintessa. 2013c. Quintessa Limited Operation Procedures Manual. Version 3.4, August 2013. Quintessa Limited, Henley-on-Thames, United Kingdom.

Quintessa. 2013d. Software Development Guidelines for Maintainable and Re-usable Code. Version 2.4, August 2013. Quintessa Limited, Henley-on-Thames, United Kingdom.

Quintessa. 2013e. AMBER 5.7 Verification Summary. Quintessa report QE-AMBER-3 Versions 5.7. Quintessa Ltd, Henley-on-Thames, UK.

Robinson. 2005 AMBER Guidance Note: Modelling Advection, Dispersion & Diffusion, November 2005.

SKB. 2010a Radionuclide transport report for the safety assessment SR-Site, SKB TR-10-50, December 2010.

SKB. 2010b Data report for the safety assessment SR-Site, SKB TR-10-52, ID 1271174n. Updated 2014-01, December 2010.

SKB. 2010c. Sources of tabulated triplets used by FARF31 (produced by ConnectFlow), SKB document ID1286751, 2010

SKB. 2010d. Model summary report for the safety assessment SR-Site, SKB TR-10-51, ID 1265002. Updated 2013-01, December 2010.

SKB. 2011. Final control of data used in radionuclide transport calculations. SKB document ID1282702, May 2011.

Walke R C and Paulley A. 2009. Preliminary Post-Closure Environmental Safety Case for the D1225 Shaft at Dounreay: Appendix E – Performance Assessment. Dounreay Site Restoration Limited report 54324/5/REP/QNT/3173/IS/01, Issue 1, March 2009.

APPENDIX 1

Coverage of SKB reports

Table 3: Summary of SKB Reports used in this Work

Reviewed report	Reviewed sections	Comments
Radionuclide transport report for the safety assessment SR-Site, SKB TR-10-50	3, 4, 6.2, 6.3, 6.5, F and G	Model specifications, details on parameter values for specific calculation cases, and model results used for comparison.
Model summary report for the safety assessment SR-Site, SKB TR-10-51	3.8, 3.9, 3.12, 3.20	Background information on SKB's modelling approach.
Data report for the safety assessment SR-Site, SKB TR-10-52	All sections.	Used to define parameter values and distributions for independent assessment models.

Summary of Compartment Modelling Approach

Dynamic processes such as radionuclide migration in groundwater (by advection or diffusion) can be effectively and accurately modelled using a compartment modelling approach. This involves representing key features as 'compartments' which are assumed to occupy a user-defined space, have particular physical properties, and in which the concentration of contaminants at a given time is uniform throughout the volume. Compartments can be linked by transfer rates that describe the fraction of the amount of a contaminant that is moved from one compartment to another in unit time. A number of transfers can operate between compartments, and the decay/ingrowth of contaminants within a compartment can also be represented. Thus, a general expression for the change in the amount of radionuclide *N* in compartment *I* with time is:

$$\frac{dN_i}{dt} = \left(\sum_{j \neq i} \lambda_{ji} N_j + \lambda_M M_i \right) - \left(\sum_{j \neq i} \lambda_{ij} N_i + \lambda_N N_i \right) \qquad 1)$$

where:

i ,j	are the two compartments;
N, M	are the amounts (Bq) of radionuclides N and M in a compartment (M is the parent of N in a decay chain);
λ_M, λ_N	are the decay constants for radionuclides M and N (y^{-1}); and
λ_{ji}, λ_{ij}	are transfer coefficients (y^{-1}) representing the gain and loss of radionuclide N from compartments i by transfer from and to compartment j, respectively.

The solution provides the time-dependent inventory of each compartment. Although a conventional compartment model essentially works in terms of total amounts of contaminants in a compartment, assumptions about compartment sizes allow estimates of the associated concentrations to be made. Transfer rates themselves can be defined in terms of other values and equations, and may be time-dependent.

A key assumption in compartment modelling is that that the distribution of contaminants within a compartment can be approximated as being uniform (either because relatively rapid mixing occurs in the compartment or because an average concentration is reasonable for the assessment purposes). If this assumption does not hold, then further discretisation may be needed (e.g. into a series of soil layers or sections of an aquifer). Care is needed to ensure that the discretisation is sufficiently refined not to add excessive numerical dispersion (Robinson, 2005).

Contaminant transport by diffusion cannot be represented directly with the general first-order expression that underlies compartment models (Equation A.1), as the rate of transport is dependent on the concentration gradient. However, it is possible to represent diffusion by using a combination of transfers between the two compartments across which diffusion occurs:

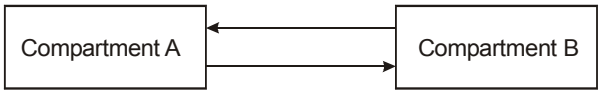

In this case, the flux of contaminants (Bq y^{-1}) in each direction can be expressed by:

$$\phi_{Diff,AB} = \frac{A\, D_{Eff}\, (C_A - C_B)}{L_{Diff}} \qquad \text{(A.2)}$$

where

A	is the area across which diffusion occurs (m^2);
D_{Eff}	is the effective diffusion coefficient (m^2 y^{-1})
C_A,C_B	is the concentration of the contaminant in compartments A and B respectively (Bq m^{-3}); and
L_{Diff}	is the diffusion length (m) (essentially the distance between the centres of each compartment, perpendicular to the face across which diffusion is occurring).

The transfer rate (y^{-1}) for diffusion can then be readily calculated by dividing each side of the equation by the amount I of the contaminant in the compartment at given time.

AMBER Model

Model Structure

The AMBER model structure is illustrated in Figure 47 to Figure 50. Figure 47 presents the three main submodels (within which compartments and transfers are defined) and the linking transfers from canister to buffer, and buffer to geosphere. Figure 48 to Figure 50 show the AMBER model compartments and transfers in each submodel in turn. In these figures, compartments are illustrated by coloured rectangles, with transfers shown as labelled arrows between them.

Figure 47: Overall AMBER Modelling Structure

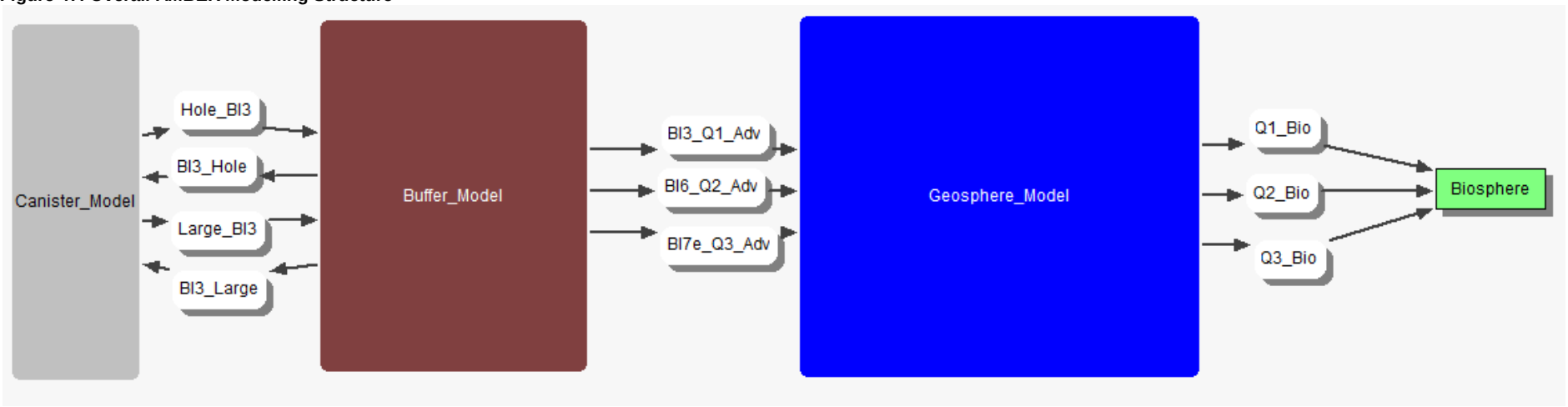

Figure 48: Canister Submodel

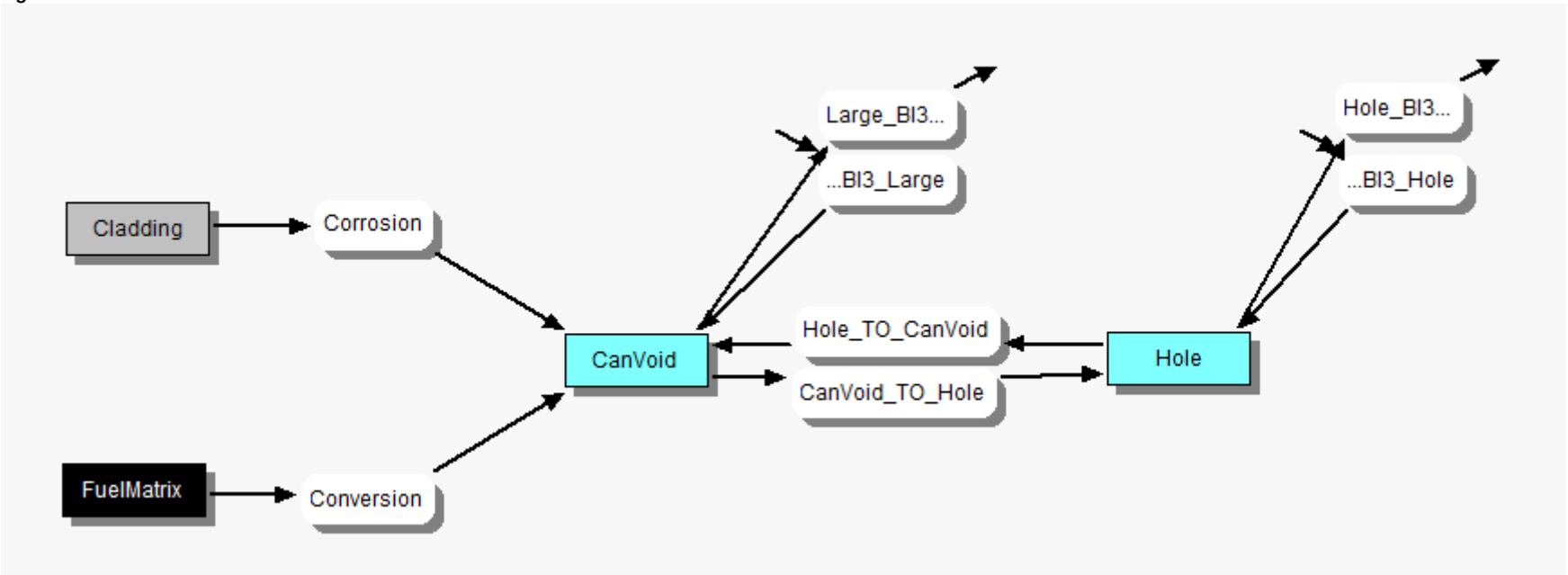

Figure 49: Buffer and Backfill Submodel

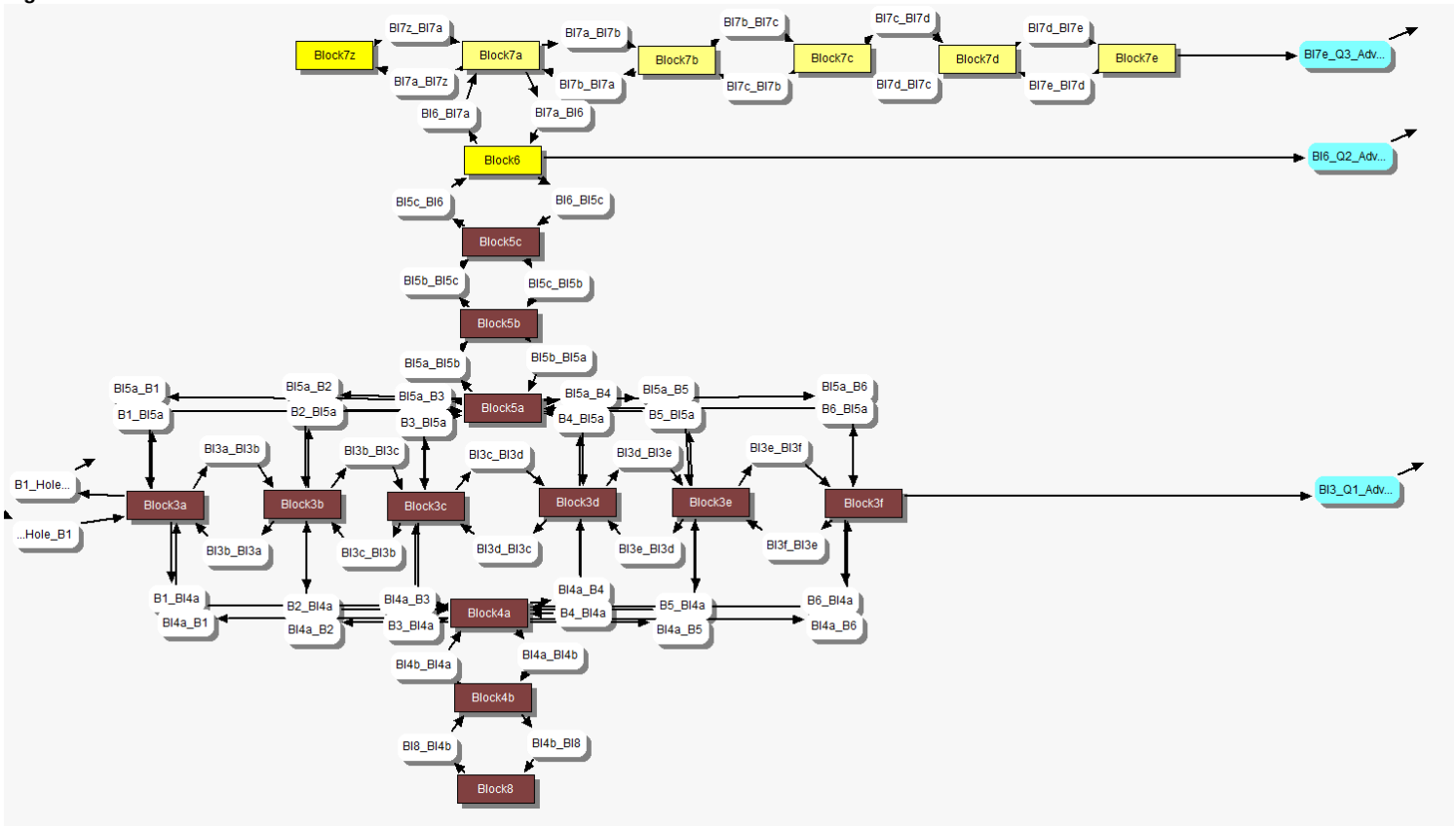

Figure 50: Geosphere Submodel – Q1 Pathway*

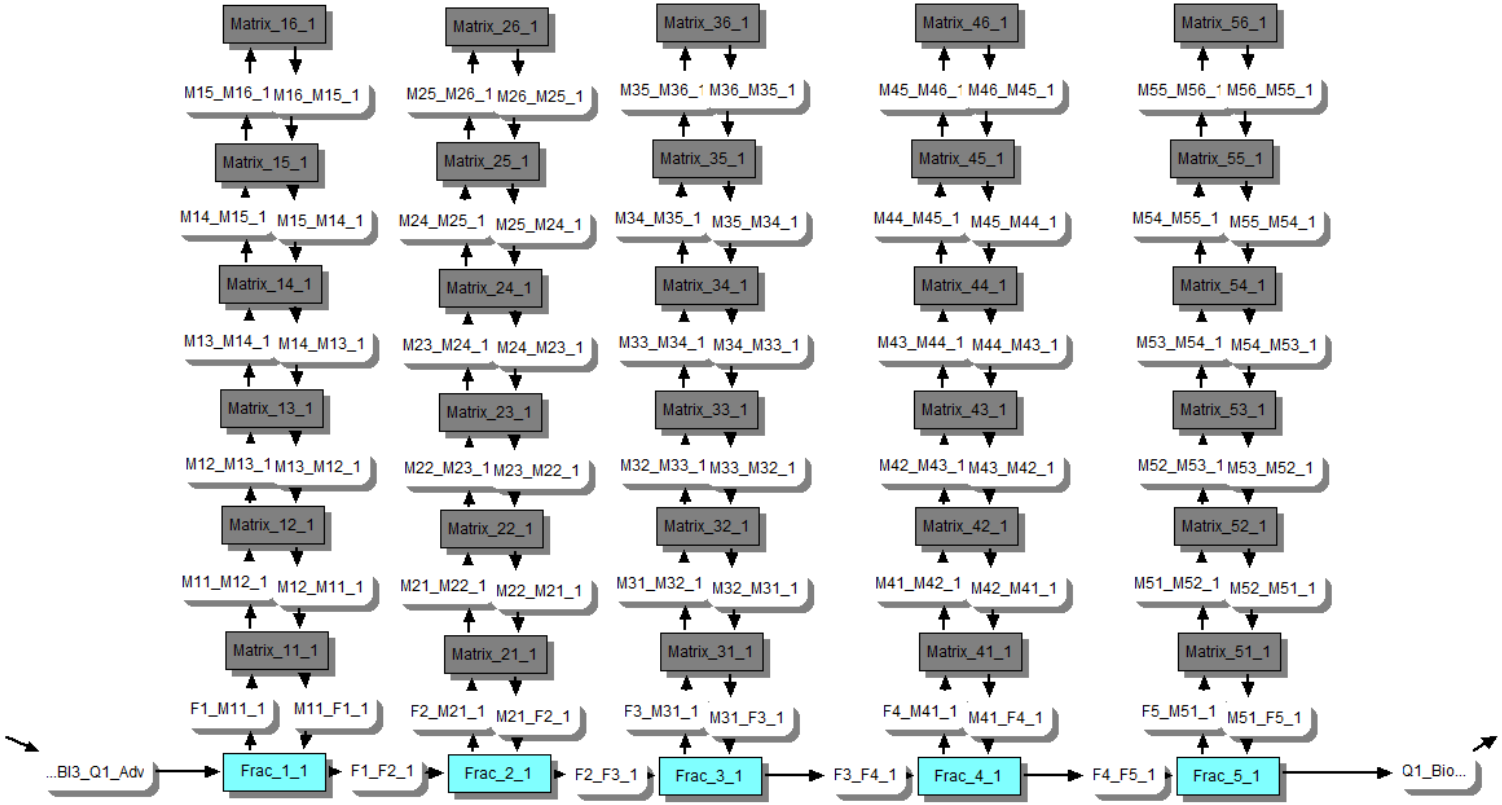

Note: * The structure of the Q2 and Q3 pathways is the same as the Q1 pathway.

AMBER Model Parameters

AMBER permits the user to define their own model parameters. The parameters used in this study are listed in this section, and have been named to reflect the nomenclature given by SKB (2012b).

A_X (m)
Compartment surface area in the x direction (or radial direction). Data are calculated from inner and outer radii (r_i and r_o) and height (L_Z) but are the same as for the buffer are from Table G.2 of SKB (2010a).

A_Z (m)
Compartment surface area in the z direction (or axial direction). Calculated from the specified inner and outer surface area (r_i and r_o).

Anion (-)
Flag to indicate if a contaminant is treated as an anion, based on Section 5.3.9 of SKB (2010a).

CRF_Median and CRF_pdf (-)
Corrosion release fraction, median value, from Table 3-4 of SKB (2010a). Parameter distributions for the corrosion release factor. This parameter defines the 'double triangle' characteristics for each relevant radionuclide, from Table 3-14 of SKB (2010b).

Capacity (m3)
The capacity for a contaminant in a compartment, taking into account sorption (calculated as volume x porosity x retardation).

D_E (m)
Depth of fracture surface available for sorption – assumed value.

D_Frac (m)
Fracture aperture, based on equation 6-18 of SKB (2010a), i.e. the travel time T_W divided by the F value.

D_p (m2/s)
Pore diffusivity in the damaged zone, defined in G-26 of SKB (2010a).

De (m2/y)
Effective diffusivity, based on various sources depending on element and calculation case. Effective diffusivity for anions and cations in buffer and backfill from Table 5-15 of SKB (2010b). Effective diffusion coefficient for anions in the rock from Table 6-91 of SKB (2010b). Median values from Table 3-3 of SKB (2010a).

F (y/m)
F value for Q1; median value from Table 3-5 of SKB (2010a).

FCR (/y)
Fuel conversion rate. The distribution is specified in Table 3-21 of SKB (2010b).

IRF (-)
Instantaneous release factors for all radionuclides. Median values of IRF from Table 3-4 of SKB (2010a) and parameter distributions for the instantaneous release factors from Table 3-15 of SKB(2010b).

Inventory (mol)
Inventory, per canister, from Table 3-7 of SKB(2010b).

Kd (m3/kg)
Sorption coefficients. Reference data for buffer and backfill relate to highly saline groundwater, from Table 5-17 and 5-19 of SKB (2010b). Buffer, backfill and rock Kd for median deterministic case from Table 3-3 of SKB (2010a).

LDF (Sv/Bq)
Landscape dose factors, taking distributed values from Table 3-7 of SKB (2010a).

L_D (m)
Thickness of matrix diffusion, from Table 6-85 of SKB (2010b).

L_Fracture (m)
Length of fracture as it intersects the hole (FLEN value). The median value is given in Table 3-5 of SKB (2010a).

L_Geo (m)
Pathlength for Q1. The median calculation takes an assumed value.

L_Hole (m)
Radius of the defect (pinhole). The size of the hole is defined in Table 4-7 of SKB (2010b).

L_M (m)
Thickness of each matrix diffusion layer, calculated from L_D, assuming six layers with each being 3 x the thickness of the previous one.

L_X (m)
Length in the radial direction (x axis). Data are from various sources: buffer values are from Table G-2 of SKB (2010a); geosphere compartments are one fifth of the geosphere pathlength (there are 5 geosphere compartments).

L_Z (m)
Length in the z axis (i.e. axial) Buffer values are from Table G-2 of SKB (2010a) and other compartments from associated descriptions.

L_i (m)
Inner radius, Table G-2 of (SKB, 2010a).

L_o (m)
Outer radius, Table G-2 of (SKB, 2010a).

R
Retardation, calculated.

Q_Eq1, Q_Eq2, Q_Eq3 (m3/y)
Equivalent flow rate for Q1, Q2 and Q3. Median values are taken from Table 3-5 of SKB (2010a).

Q_Eq1DZ (m3/y)
Flow through the damaged zone, from the equation defined as G-26 in SKB (2010a).

Sol (mol/m3)
Solubility limits. Median values are taken from Table 3-4 of SKB (2010a), sampled data taken from file.

T_W (y)
Travel time for Q1. The deterministic value is obtained from Table 3-5 of SKB (2010a).

U_0 (m/y)
Darcy velocity for Q1. The median value is defined in Table 3-5 of SKB (2010a).

V_Can (m3)
Void volume of average canister, from Table 4-4 of SKB (2010b).

V (m3)

Volume of compartment, calculated.

W_Zone (m)
Width of the damaged zone, defined in Equation G-26 of SKB (2010a).

d_Zone (m)
Thickness of the damaged zone, defined in Equation G-26 of SKB (2010a).

lambda_Adv (/y)
Advective transport rate - calculated.

lambda_Corr (/y)
Rate of release via corrosion, calculated.

lambda_Diff_x (/y)
Diffusion rate in the x/radial direction, calculated.

lambda_Diff_z (/y)
Diffusion rate in the z/axial direction, calculated.

lambda_FCR (/y)
Fuel conversion transfer, calculated.

lambda_Frac (/y)
Transport into the Q1 fracture, calculated.

lambda_Hole (/y)
Transfer rate from canister to hole, calculated.

q (m3/s)
Water flow rate of the damaged zone, defined in Equation G-27 of SKB (2010a).

q_Frac (m/y)
Transport velocity in fractures, calculated from length of geosphere divided by travel time.

r_f (y/m3)
Plug resistance for fracture. Data are specified in Section G (after Equation G-3) of SKB (2010a).

r_p (y/m3)
Plug resistance of the canister hole; equation G-1 of SKB (2010a).

rho (kg/m3)
Dry bulk density. Data for buffer and backfill are from Table 5-5 and 5-6 of SKB (2010b) and data for rock from Table 6-50 of SKB (2010b).

t_Corr (y)
Corrosion time, used to derive the corrosion release rate. The parameter distribution is defined in Table 3-18 of SKB (2010b). Fast corrosion is assumed for case E.

t_Delay (y)
Delay time for onset of radionuclide transport. Values are defined in Section 4.2.10 of SKB (2010b) and Section 6.5 of SKB (2010a).

t_Large (y)
Time at which there is a large breach of the canister. Values are defined in Section 4.2.10 of SKB (2010b) and Section 6.5 of SKB (2010a).

theta (-)

Porosity. Data are from Table 5-5 and 5-6 of SKB (2010b) for buffer and backfill, with values for rock from Table 6-90 of SKB (2010b) and the damaged zone from Equation G-26 of SKB (2010a).

2014:55

The Swedish Radiation Safety Authority has a comprehensive responsibility to ensure that society is safe from the effects of radiation. The Authority works to achieve radiation safety in a number of areas: nuclear power, medical care as well as commercial products and services. The Authority also works to achieve protection from natural radiation and to increase the level of radiation safety internationally.

The Swedish Radiation Safety Authority works proactively and preventively to protect people and the environment from the harmful effects of radiation, now and in the future. The Authority issues regulations and supervises compliance, while also supporting research, providing training and information, and issuing advice. Often, activities involving radiation require licences issued by the Authority. The Swedish Radiation Safety Authority maintains emergency preparedness around the clock with the aim of limiting the aftermath of radiation accidents and the unintentional spreading of radioactive substances. The Authority participates in international co-operation in order to promote radiation safety and finances projects aiming to raise the level of radiation safety in certain Eastern European countries.

The Authority reports to the Ministry of the Environment and has around 315 employees with competencies in the fields of engineering, natural and behavioural sciences, law, economics and communications. We have received quality, environmental and working environment certification.

Strålsäkerhetsmyndigheten
Swedish Radiation Safety Authority

SE-171 16 Stockholm
Solna strandväg 96

Tel: +46 8 799 40 00
Fax: +46 8 799 40 10

E-mail: registrator@ssm.se
Web: stralsakerhetsmyndigheten.se